Supplementary information for

Less chemicals for more controlled syntheses: on the benefits of mixtures of alcohols for room temperature surfactant-free colloidal syntheses of gold nanoparticles

Julie Christine Hamer Larsen,[a,†] Astrid Nymann Porsgaard,[a,†] Leander Vinding,[a,†]
Aleksandra Smolska,[a] Jonathan Quinson [a,*]

a) Nanomaterials Engineering for Sustainable Technologies (NEST) group,
Biological and Chemical Engineering Department,
Aarhus University, 40 Åbogade, 8200 Aarhus, Denmark

† Equally contributing authors

* corresponding author: jquinson@bce.au.dk, ORCID: 0000-0002-9374-9330

Contents

1. Literature

Table S1. Relative pros and cons of glycerol and ethanol for RT surfactant-free colloidal syntheses of Au NPs. In green are desirable general features for controlling the Au NPs properties such as size, general consideration for processing the material and reproducibility.

Feature	**Ethanol**	**Glycerol**	**Ref.**
Overall kinetics*	Slower	Faster	[1]
Size	Larger	Smaller	[1]
Size distribution	Broader	Narrower	[1]
Robustness**	Lower	Higher	[1]
Viscosity	Lower	Higher	[2,3]
Stability	Long	Long	[4]

* Based on the appearance of a red color characteristic of small size 5-10 nm Au NPs evaluated by the naked eye. ** Considered as the width of experimental window where the synthesis is successful, i.e. formation of small size and stable Au NPs when different amounts of base and/or alcohol contents and/or different light environments are used.

2. Materials methods

1.1. Chemicals

All chemicals were used as received: $HAuCl_4 \cdot 3H_2O$ (99%, BLD Pharmatech); NaOH (Reag. Ph. Eur., VWR); ultrapure water (mQ, Milli-Q, Millipore, resistivity of >18.2 MΩ•cm); ethanol (Et, ≥99.8%, AnalaR NORMAPUR® ACS, Reag. Ph. Eur. analyse reagens, VWR); methanol (Met, AnalaR NORMAPUR, Reag. Ph. Eur. ACS, VWR); glycerol (Gly, bi-distilled 99.5%, VWR); HCl (puriss. ACS reagent, reag. ISO, Reag. Ph. Eur. fuming, ≥ 37%, Sigma Aldrich); HNO_3 (puriss ≥ 65%, Sigma Aldrich). None of the chemicals was in contact with metal (plastic spatula were preferred to handle the solids).

Note: the synthesis proceeds well with lower grade chemicals,[5,6] although the effect(s) of industrial grade materials is pending (e.g. renewable ethanol from crops or sugar cane or other agricultural waste or non-food sources).

1.2. Synthesis

The general principles and protocols for alcohol-mediated syntheses have been described elsewhere [1,2,4,6-9]. The synthesis of the Au NPs is performed by adding $HAuCl_4$ to a mixture of water, NaOH and an alcohol. The reaction proceeds at RT without the need for extra chemicals to lead to colloidal dispersions of Au NPs stable for months [1]. The synthesis is scalable [7]. The synthesis is best performed using high purity water [6]. The synthesis is best performed by adding $HAuCl_4$ last from a relatively concentrated solution of $HAuCl_4$ (at 50 mM in mQ water in this work, stored in the fridge) [1,7]. The base is best used from stock solution stored in a plastic container (at 50 mM in mQ water in this work, stored at RT) [9]. The synthesis is best performed under controlled light environment [1]. Although the synthesis does not require stirring [3,7,10], more reproducible results are obtained using magnetic stirring (PTFE cylindrical stirrer bar, 8 x 3 mm, VWR, 442-4520) and the magnets used were cleaned with *aqua regia* (4:1, v:v, HCl:HNO_3; to be handled and disposed of with care following the related safety procedures in place in the laboratory).

As schematized in **Scheme S1**, and to comply with the principles of sustainable laboratory practices and thus limit the volume of waste generated, the reaction was performed in disposable 1 cm wide rectangular polystyrene (PS) UV-vis cuvettes (340-900 nm, VWR, 634-0675) containing a magnet (unless otherwise specified), de-dusted with a flow of compressed air prior to the addition of the chemicals. The chemicals were added from the stock solutions (NaOH: 50 mM in mQ, $HAuCl_4$: 50 mM in mQ, ethanol as received, methanol as received, glycerol from a 60 v.% stock solution in mQ to facilitate the handling of this otherwise viscous chemical, only the experiments using 3.3 v.% glycerol where obtained using pure glycerol as stock solution) in the order water < base < alcohol(s) < $HAuCl_4$.[7]. $HAuCl_4$ was added last [7], under stirring in a photo-box (Puluz LED portable Photo Studio, PU5060EU, 60 cm x 60 cm x 60 cm, 60 W) to control the light environment [1,6,7]. The samples were capped with dedicated stoppers and left to react for 2 hours in the photo-box with stirring. Alternatively, the samples were subjected to a 365 nm light (OFK-8000 OptimaxTM Multi-LiteTM inspection kit, Spectroline), illuminated from the top and without capping, for 2 hours, as described elsewhere [1], or kept under dark conditions for 2 hours (capped) using aluminum foil. The samples were then left for a day at RT and ambient light without stirring. The samples were then stored at RT in a drawer.

The final concentrations before taking into account volume contraction were typically 80 v.% water and 20 v.% alcohols in total, unless otherwise specified. The alcohols were ethanol (alternatively methanol) and/or glycerol in the indicated v.% (expressed before taking into account volume contraction that can happen in alcohol-water mixtures such as ethanol-water mixtures due to hydrogen bonding). The other parameters were fixed as per optimal conditions previously established for ethanol-mediated syntheses [1,4,7], i.e. 2 mM NaOH and 0.5 mM $HAuCl_4$ for a total volume of 2 mL (before taking into account volume contraction). A NaOH/Au molar ratio of 4 was previously established as an optimal value in light of the equation of the reduction process [7]. An overview and summary of the samples considered and their characteristics is provided in **Table S3**.

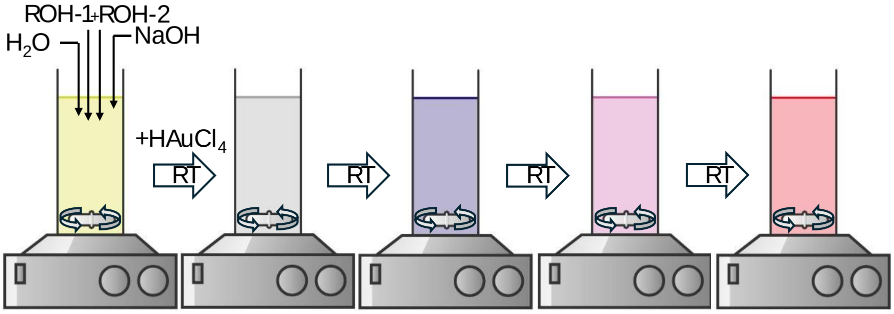

Scheme S1. Illustration of the room temperature (RT) synthesis of surfactant-free colloidal Au NPs mediated by alcohols (ROH) under alkaline conditions. Diagram(s) created with Chemix (2025). Retrieved from https://chemix.org and adapted.

1.3. *Characterization*

A focus for this study is given to the properties retrieved from UV-vis measurements because UV-vis spectra are very informative when it comes to plasmonic Au NPs [8]. The characterization is completed by scanning transmission electron microscopy (STEM). To develop more sustainable research [11], it will not be realistic to use all characterization methods reported for Au NPs [12,13] for all the samples obtained here with a relatively high throughput [4]. Further characterization of the surfactant-free fcc Au NPs by XPS, XRD, X-ray total scattering with PDF analysis, high resolution TEM or zeta-potential measurements can be found elsewhere [7].

1.3.1. UV-vis spectroscopy

Metrics. The Mie theory correlates various variables to the optical properties of Au NPs [14-16]. UV-vis spectra of Au NPs result from a complex interplay between the properties of gold, nanoscale effects (such as size and shape) and interaction with the solvents and/or interactions between NPs and precursor [17]. Due to their plasmonic properties (surface plasmon resonance, spr), several relevant parameters descriptive of the Au NPs can be retrieved: λ_{spr} [16], A_{400} [14], A_{spr}/A_{450} [16], A_{380}/A_{800} [18], all defined, detailed and summarized in **Table S2**. Note that the relationships indicated are only true for certain conditions that are not always met in the experiments below (e.g. for low yields experiments or for too large NPs) but are convenient indicators of the properties of the Au NPs. The good correlation between λ_{spr} values and size retrieved by STEM is detailed elsewhere [1] and documented in **Figure S3**.

Table S2. Various metrics retrieved from UV-vis for Au NPs.

Metric	Description	Property	Trend	Ref
λ_{spr} (nm)	Wavelength at the maximum of absorption	Surface plasmon resonance (spr)	Lower values ➔ smaller NPs	[16]
A_{400} (a.u.)	Absorption at 400 nm (typically normalized)	(Relative) Yield of the synthesis	Higher values ➔relatively higher yields	[14]
A_{spr}/A_{450}	Ratio of the absorbance at the spr and at 450 nm	Relates to NP size	Lower values ➔ smaller NPs	[16]
A_{380}/A_{800}	Ratio of the absorptions measured at 380 and 800 nm	Stability of the colloids	Higher values ➔ more stable colloids	[18]

For kinetics studies, A_{max} corresponds to the maximum of absorption and for the dataset here is in most cases such that A_{max}=A_{spr}. Although at the initial stages of the reaction no clear spr signal is observed, A_{max} is representative of the overall absorption since the spectra are almost straight lines. The value $\sqrt[3]{A_{max}}$ when A_{max}=A_{spr} is proportional to $\sqrt[3]{N}R$, where R is the radius of the NP and N is the number of NPs [17].

Samples. UV-vis spectra were acquired using a Shimadzu UV-1800 UV/Visible scanning spectrophotometer typically between 290 and 800 nm. As baseline, a solution with the corresponding amount of mQ water and the corresponding amount of ethanol or methanol and/or glycerol to what was used in the sample were preferred (no base, no $HAuCl_4$). All samples were measured the day after synthesis (although it is important to note that the samples are stable for months, see **Section 8** below). The samples are prepared directly in UV-vis cuvettes that were also used for those measurements.

Kinetics. For kinetics study the samples were measured for 2 hours in such a way that the sample in a UV-vis cuvettes as described above was directly placed in a UV-vis Go Direct® SpectroVis® Plus spectrophotometer with a fixed scan range of 380 nm to 950 nm. It takes only ca. 1-2 seconds to acquire the whole range. However, measurements below 400 nm and above 800 nm proved to be unreliable. Due to the relatively low resolution of the measurement, the data were then filtered prior to analysis using the *Signal Processing Feature* of the Origins software and the *Adjacent*

Averaging method with a *Point of Windows* equal to 18, see **Figure S1**. The background was a mixture of alcohol and water together with the base with the same alcohol, alcohol content, base and base concentration as the sample considered. The background acquisition and the actual measurements were under stirring in a photo-box (Puluz LED portable Photo Studio, PU5060EU, 60 cm x 60 cm x 60 cm, 60 W). $HAuCl_4$ was added last. Spectra were recorded every 30 seconds with a first spectra 15 seconds after $HAuCl_4$ was added.

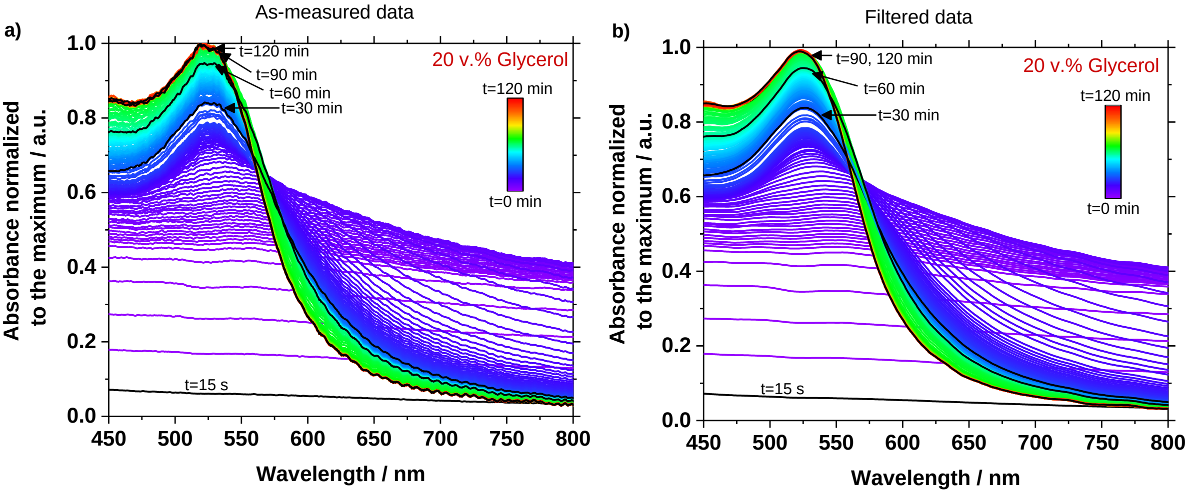

Figure S1. UV-vis spectra for kinetic experiments. (a) Raw as-measured data and (b) filtered data with the example of a sample obtained with 20 v.% glycerol. 0.5 mM $HAuCl_4$ and 2 mM NaOH were used in all cases. The spectra corresponding at times 15 s, 30 min, 60 min and 120 min are highlighted in dark and with arrows (90 and 120 min spectra overlap).

1.3.2. STEM

A FEI Talos F200X operated at 200 kV, equipped with a high-angle annular dark-field (HAADF) detector was used for electron microscopy characterization. STEM mode was preferred for a better contrast in the micrograph for size estimation. The as-prepared colloidal dispersions were dropped on copper TEM grids (Sigma-Aldrich), placed on an absorbing filter paper. The solvent was left to evaporate. The samples were characterized by imaging at least 3 randomly selected areas at 3 different magnifications. Typically, at least 100 NPs were used to estimate the diameter of the NPs (N values reported below correspond to the number of NPs counted). The ImageJ software was used for size analysis.

Table S3. Overview of the Au NP samples and properties. All experiments were performed with 0.5 mM $HAuCl_4$ and 2 mM NaOH. The Figures and sections of the manuscript where the data are used and displayed are indicated.

Ethanol v.%	**Glycerol** v.%	**Total alcohol** v.%	**λ_{spr}** nm	**A_{400}/A_{400_max}** -	**A_{spr}/A_{450}** -	**A_{380}/A_{800}** -	**Diameter** nm
Figure 2, Figures S2-S4, S8							
1	0	1	589*	0.029	1.25	2	N/A
2	0	2	584*	0.083	1.16	2	N/A
10	0	10	558	0.732	1.35	2	18.6 ± 12.1
18	0	18	526	0.996	1.76	21	16.5 ± 4.4
19	0	19	524	0.938	1.64	12	12.1 ± 4.5
20	0	20	524	1.000	1.69	22	13.8 ± 3.9
0	1	1	555	0.437	1.23	2	22.1 ± 9.7
0	2	2	542	0.767	1.76	9	21.2 ± 9.8
0	10	10	522	0.958	1.62	36	9.5 ± 2.9
0	18	18	520	0.978	1.57	38	8.2 ± 2.7
0	19	19	522	0.983	1.63	37	9.3 ± 3.4
0	20	20	518	0.991	1.51	30	8.0 ± 2.5
19	1	20	524	0.984	1.77	104	16.7 ± 5.3
1	19	20	519	0.987	1.53	31	8.5 ± 2.7
18	2	20	521	0.97	1.58	31	7.5 ± 2.8
2	18	20	523	0.994	1.64	38	8.9 ± 2.9
10	10	20	518	0.98	1.47	55	7.2 ± 2.1
Figure 3, Figures S5-S7, S9 - Regular light conditions							
20	0	20	523	0.80	1.53	7	11.5 ± 4.7
19.5	0.5	20	521	0.94	1.62	26	-
19	1	20	519	0.95	1.57	25	8.6 ± 2.8
18	2	20	518	0.95	1.53	26	-
17	3	20	518	0.93	1.53	32	7.3 ± 2.3
16	4	20	517	0.97	1.50	27	-
15	5	20	516	0.85	1.45	25	-
10	10	20	516	0.87	1.42	29	6.4 ± 1.6
5	15	20	516	0.88	1.39	29	-
0	20	20	516	0.89	1.41	29	-
10	0	10	528	0.88	1.50	2	24.3 ± 6.8
0	10	10	518	0.88	1.51	32	7.2 ± 1.9
Figures S6-S7 – Blue light conditions + Dark							
20	0	20	526	0.98	1.70	14	-
19.5	0.5	20	523	0.88	1.65	23	-
19	1	20	522	0.87	1.61	26	-
18	2	20	523	0.89	1.62	30	-
17	3	20	520	0.86	1.57	30	-
16	4	20	521	0.88	1.58	30	-
15	5	20	519	0.99	1.54	30	-
10	10	20	519	0.99	1.53	62	-
5	15	20	515	1.00	1.37	26	-
0	20	20	519	0.97	1.51	31	-
20	0	20	528	0.93	1.49	2	-
Figure S10-S11 – Kinetics							
20	0	20	528	0.97	1.55	4	8.2 ± 2.2
18	2	20	518	0.97	1.44	16	7.7 ± 3.0
0	20	20	519	1.00	1.50	32	11.0 ± 4.3
Figure 5, Figures S15-S17 – Optimization							
3	0	3	560	0.29	1.05	2	-
5	0	5	543	0.50	1.21	2	-
8	0	8	558	0.31	1.06	2	-
10	0	10	522	0.92	1.42	3	-
			524	0.92	1.47	5	8.0 ± 6.7
3	2	5	518	0.87	1.46	25	-
			520	0.92	1.48	24	5.5 ± 1.4
8	2	10	520	0.93	1.41	17	-
			519	0.92	1.44	20	5.5 ± 1.5
8	3.3	11.3	516	1	1.38	14	-
0	3.3	3.3	557	0.43	1.18	2	-
0	2	0	519	0.86	1.57	38	-
			525	0.86	1.62	27	11.7 ± 3.6

* For those samples the spr peak is very broad as detailed in **Figure 2** and the materials obtained are not stable as colloids, therefore no STEM analysis was performed.

3. UV-vis characterization

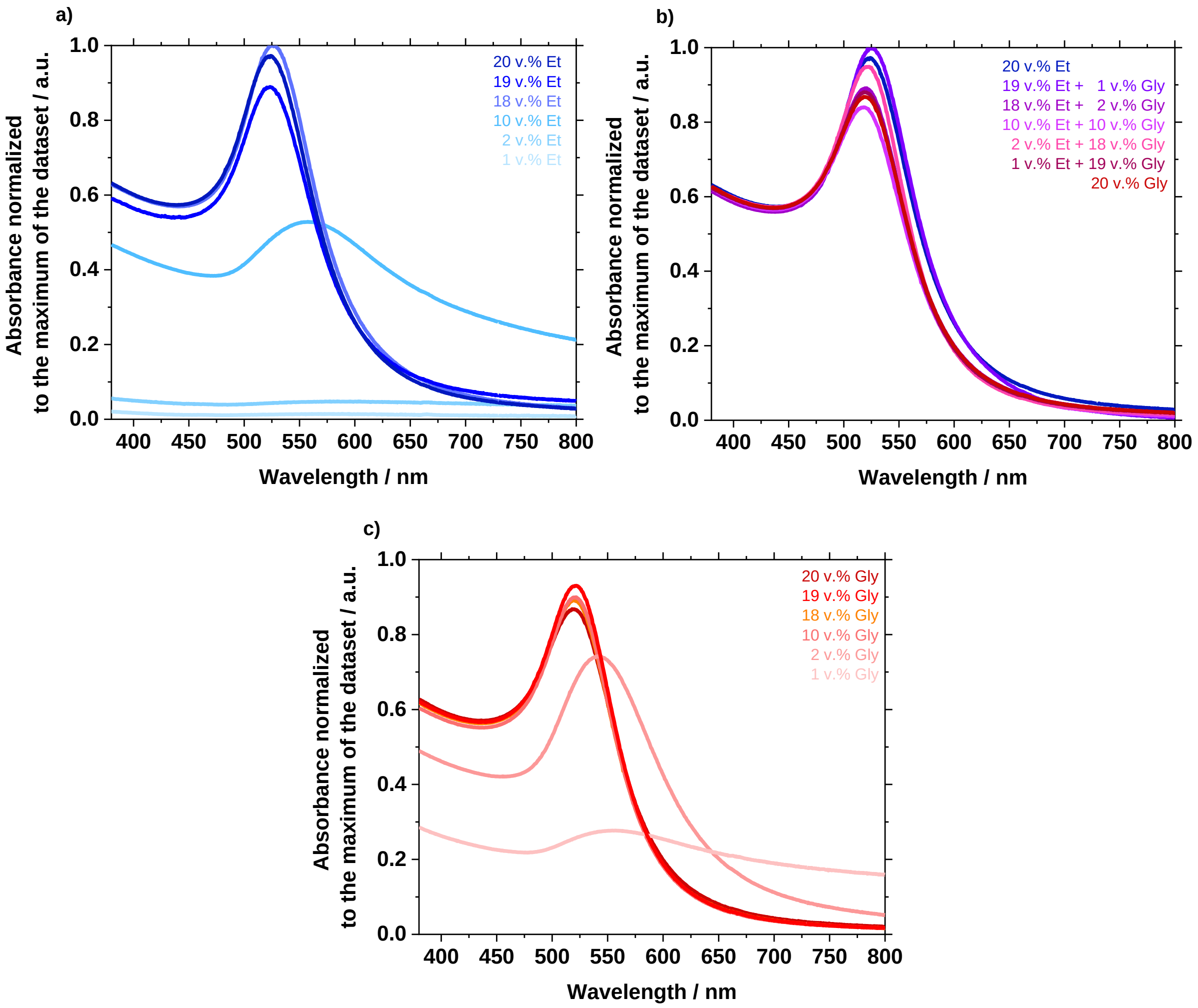

Figure S2. (a-c) UV-vis spectra for various samples, as indicated, using as source of reducing agent (a) ethanol only in various contents, (b) [ethanol+glycerol] in various ratios and (c) glycerol only in various contents, as indicated.

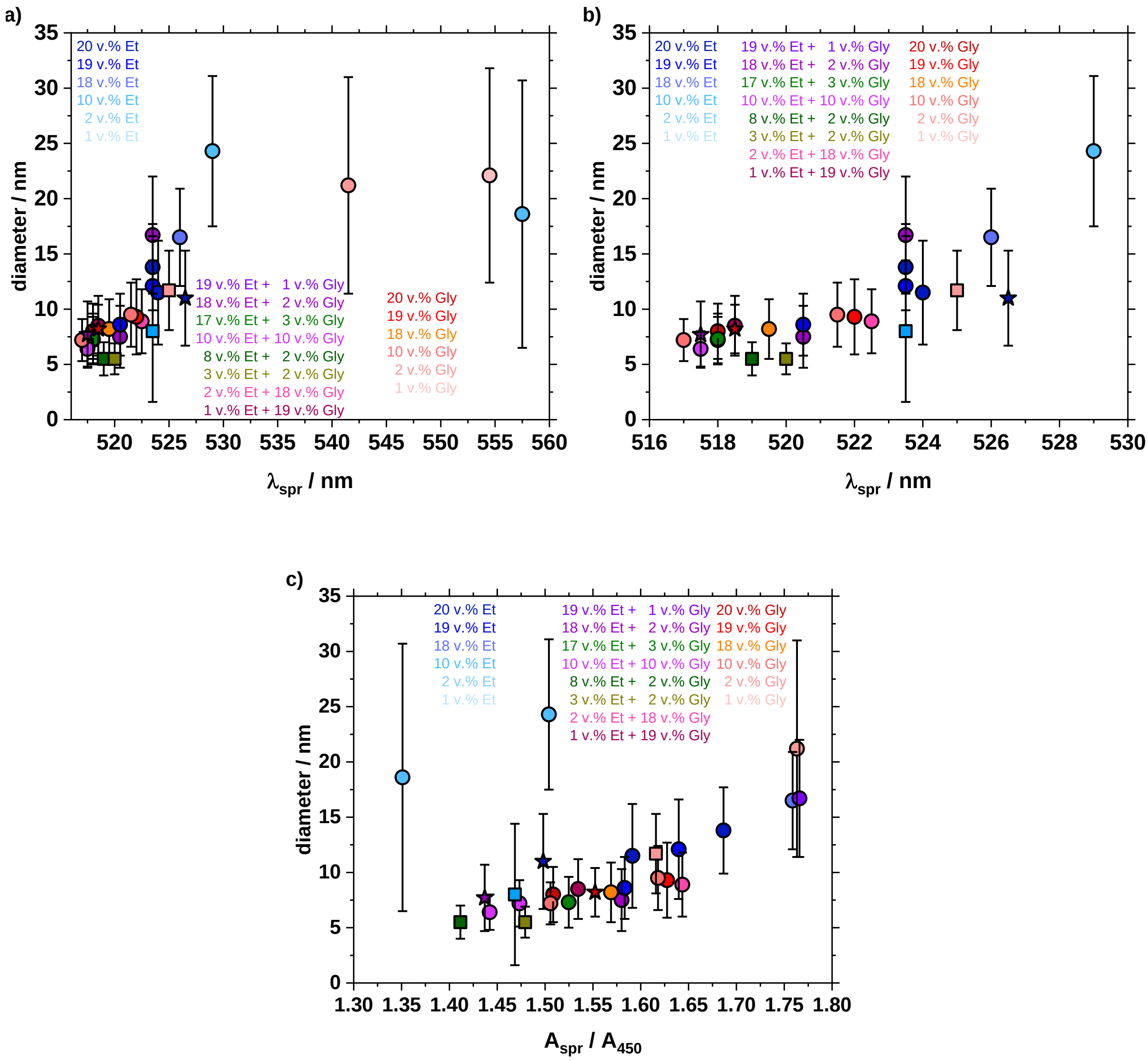

Figure S3. Relationships between UV-vis metrics and size retrieved from STEM analysis. (a, b) diameter of the NPs as a function of λ_{spr} and (c) as a function of A_{spr}/A_{450}, for various samples, as indicated. The round (○) data points correspond to data points from Figure 2, Figures S5-S9. The star (☆) data points corresponds to the data retrieved from kinetic experiments, Figures S10-S11. The square (□) data points correspond to data points from Figure 5, Figures S15-S17.

Overall, across the different experimental conditions studied here, the synthesis leads to spherical Au NPs of various sizes with examples given in **Figure 1** of the main manuscript and for which STEM data are presented in **Section 4**. It is worth pointing out that low A_{spr}/A_{450} values correspond well to smaller size NPs only when the spr peak is well-defined.

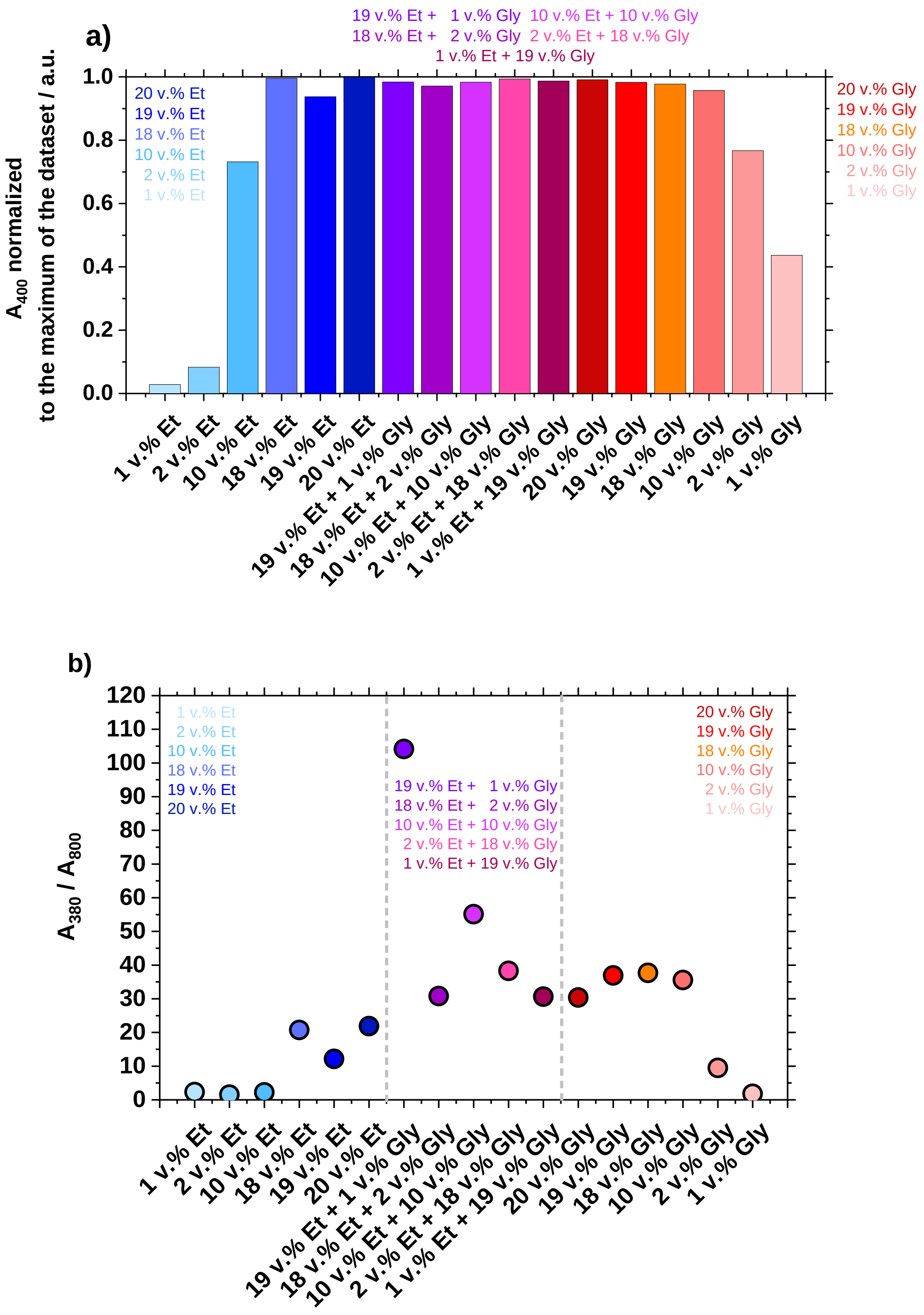

Figure S4. (a) A_{400} (normalized) and (b) A_{380}/A_{800} values for various samples, as indicated. 0.5 mM $HAuCl_4$ and 2 mM NaOH were used in all cases. Et: Ethanol; Gly: Glycerol.

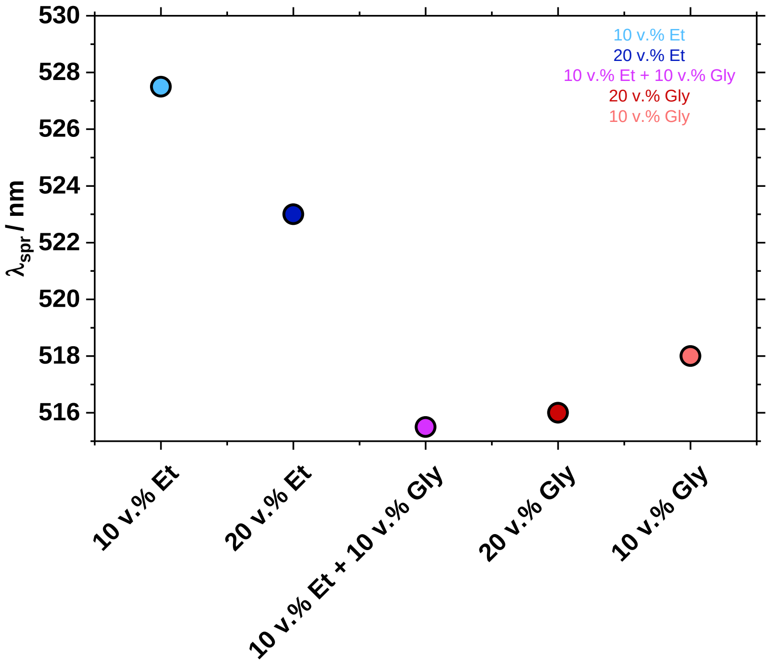

Figure S5. λ_{spr} retrieved from UV-vis characterization as a function of different alcohol contents and mixtures, as indicated, for repeated experiments (different dataset than in Figure 2 in the main manuscript). 0.5 mM $HAuCl_4$ and 2 mM NaOH were used in all cases. Et: Ethanol; Gly: Glycerol.

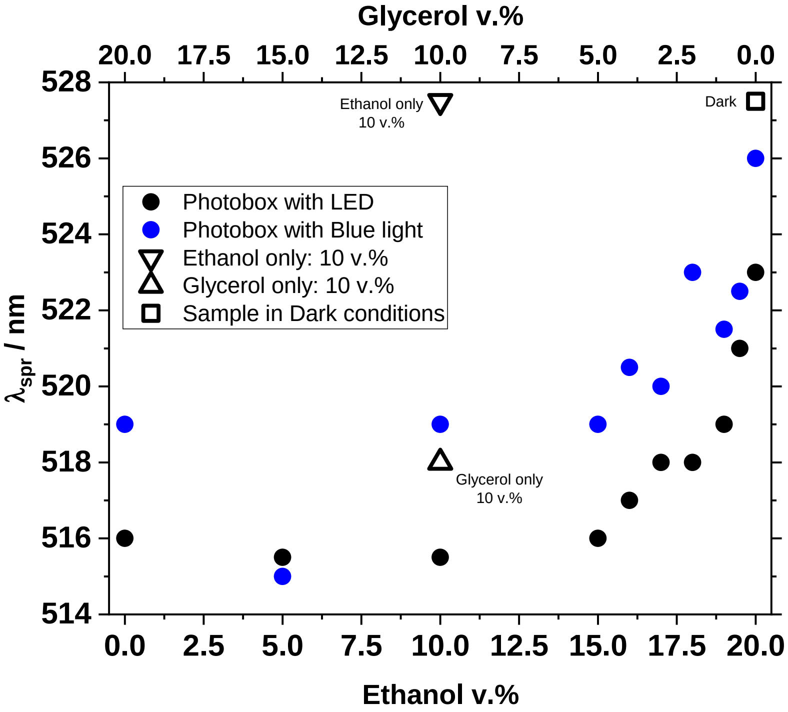

Figure S6. λ_{spr} values retrieved from UV-vis characterization as a function of different alcohol contents and mixtures, as indicated, for repeated experiments (different dataset than in Figure 2 in the main manuscript). Unless otherwise specified the total amount of alcohol was 20 v.%. The data points in black are the same as for Figure 3 in the manuscript and are reported for comparison. Different light conditions were used, as indicated. The Dark conditions were obtained by wrapping the samples in aluminum foil after adding $HAuCl_4$. Unless otherwise specified the total amount of alcohol was 20 v.%, 0.5 mM $HAuCl_4$ and 2 mM NaOH were used in all cases.

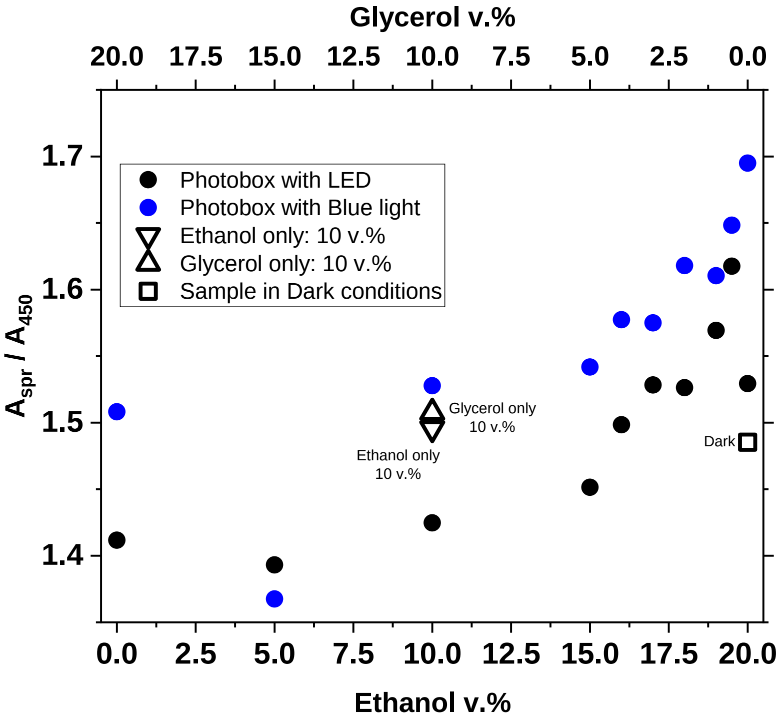

Figure S7. A_{spr}/A_{450} values retrieved from UV-vis characterization as a function of different alcohol contents and mixtures, as indicated, for repeated experiments (different dataset than in **Figure 2** in the main manuscript). Unless otherwise specified the total amount of alcohol was 20 v.%. Different light conditions were used, as indicated. The Dark conditions were obtained by wrapping the samples in aluminum foil after adding $HAuCl_4$. Unless otherwise specified the total amount of alcohol was 20 v.%, 0.5 mM $HAuCl_4$ and 2 mM NaOH were used in all cases.

4. STEM characterization

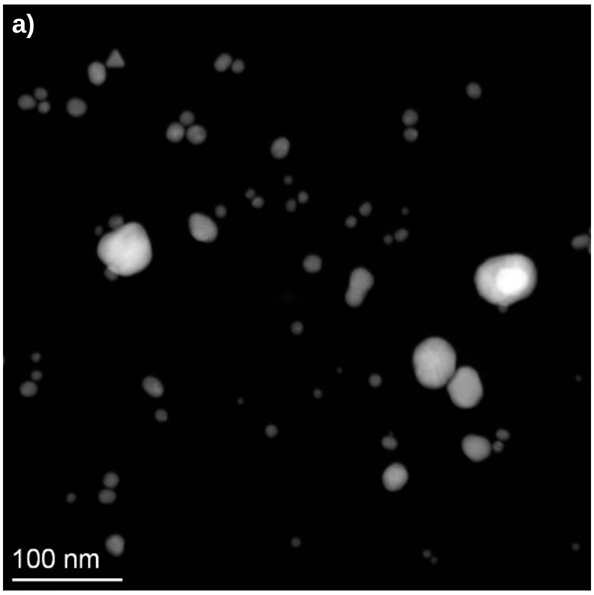

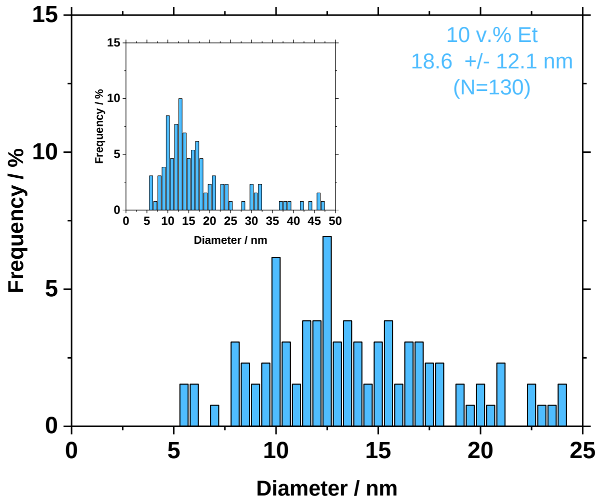

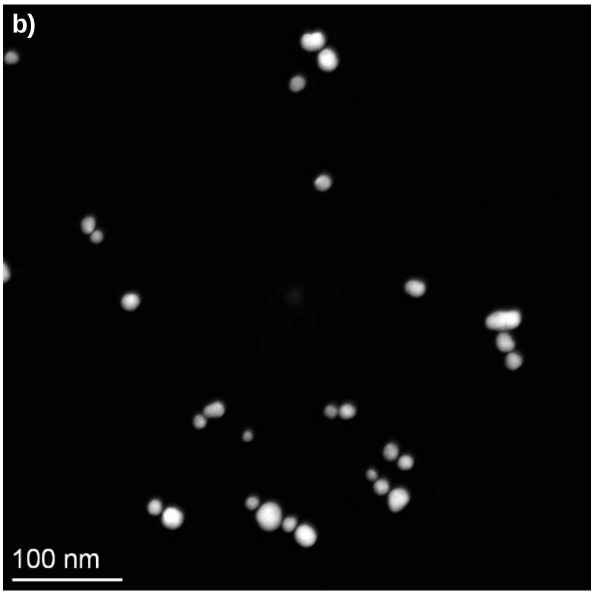

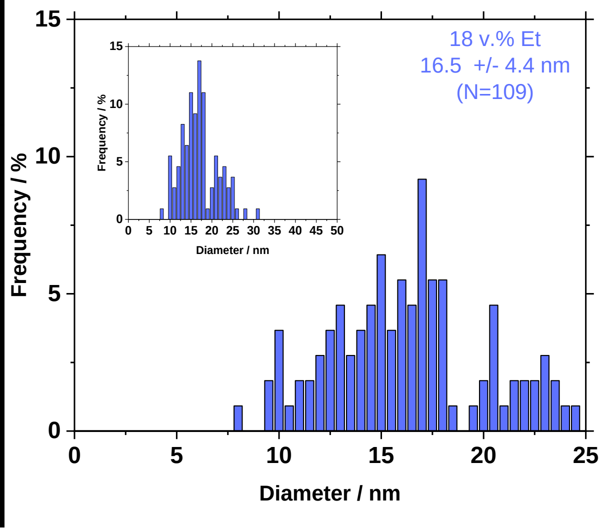

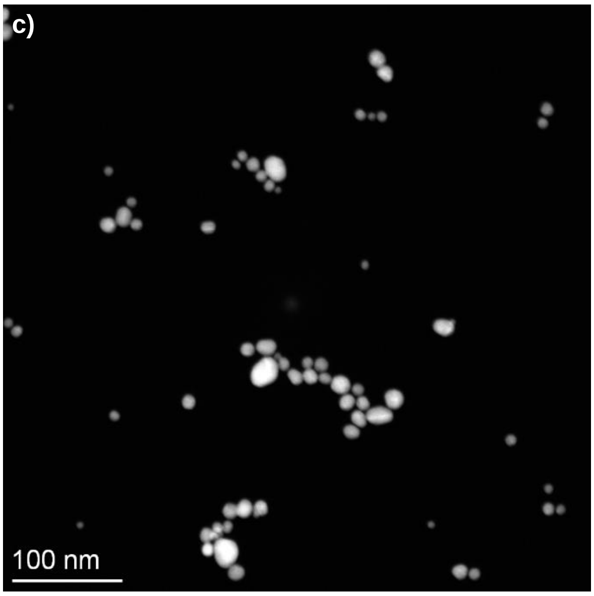

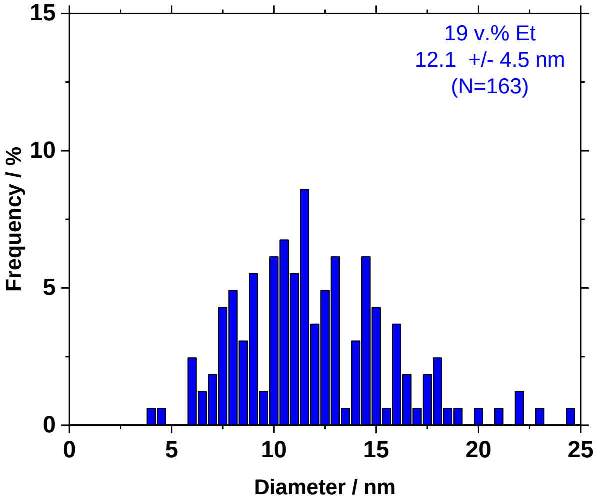

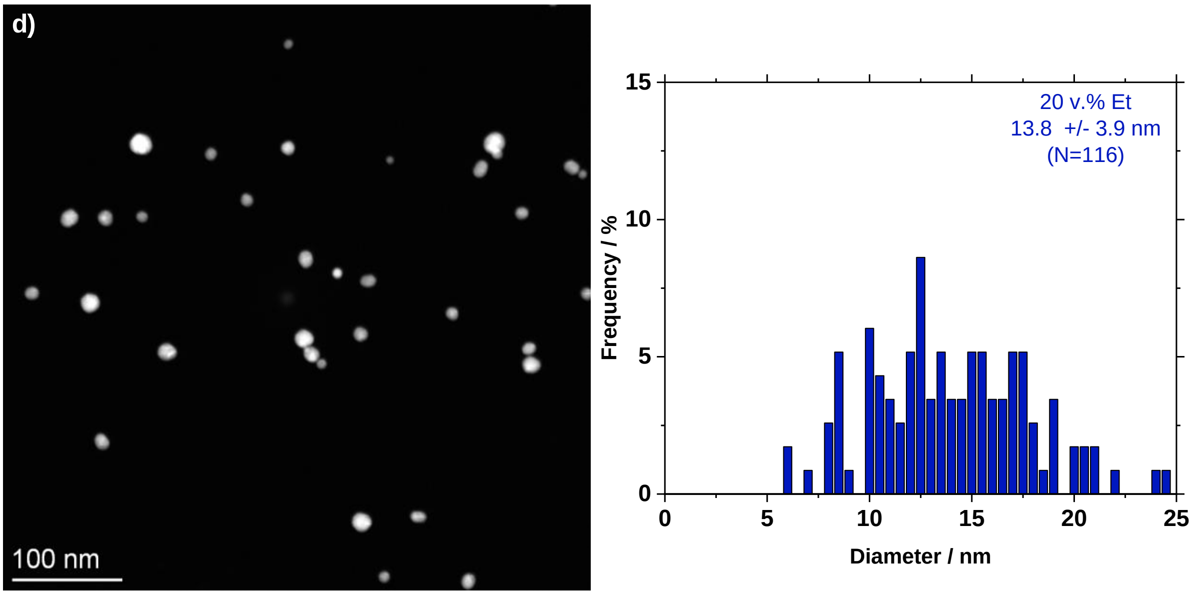
d)
100 nm
20 v.% Et
13.8 +/- 3.9 nm
(N=116)
Frequency / %
0
5
10
15
Diameter / nm
0
5
10
15
20
25

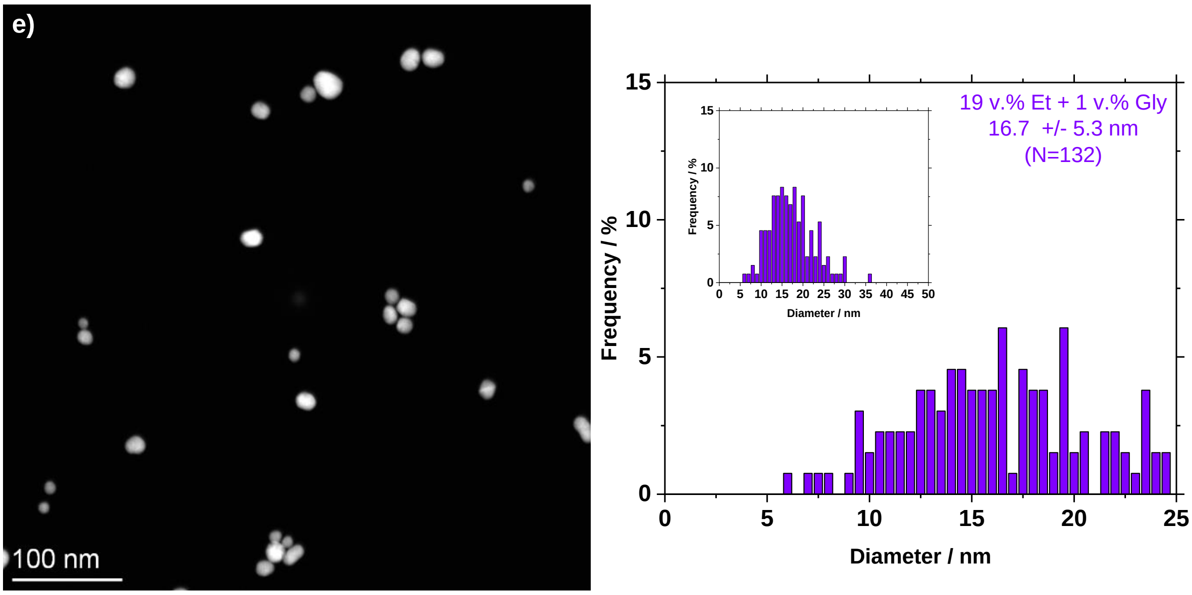
e)
100 nm
19 v.% Et + 1 v.% Gly
16.7 +/- 5.3 nm
(N=132)
Frequency / %
0
5
10
15
Diameter / nm
0
5
10
15
20
25
0
5
10
15
20
25
30
35
40
45
50

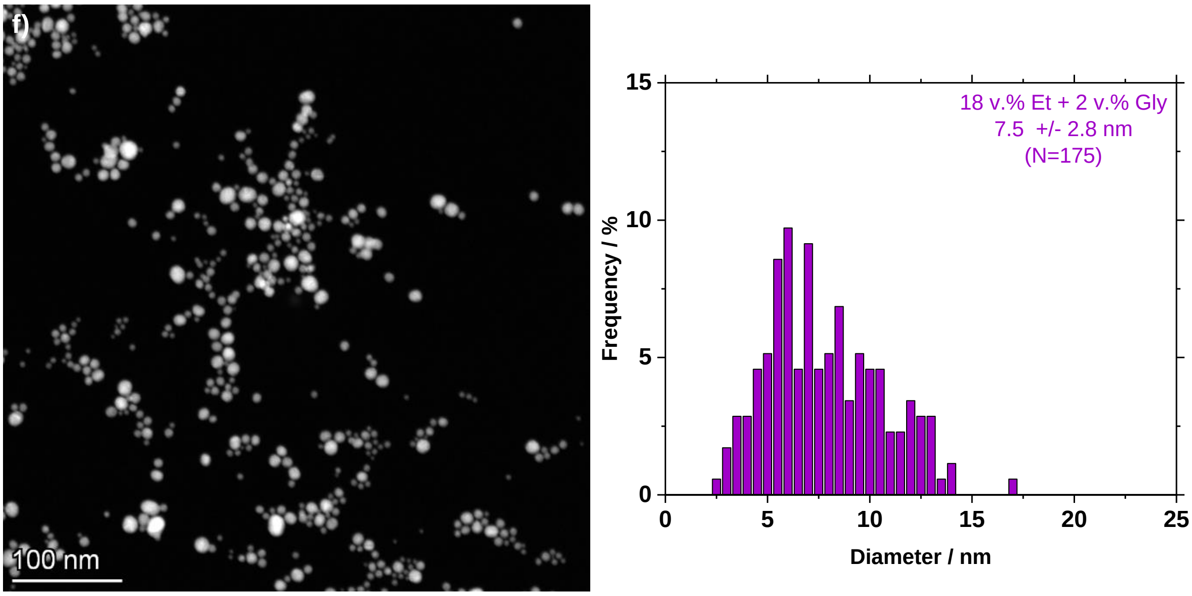
f)
100 nm
18 v.% Et + 2 v.% Gly
7.5 +/- 2.8 nm
(N=175)
Frequency / %
0
5
10
15
Diameter / nm
0
5
10
15
20
25

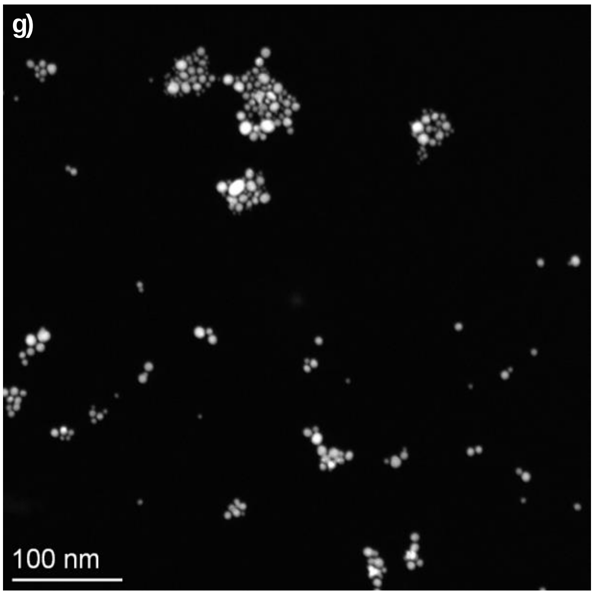
g)
100 nm

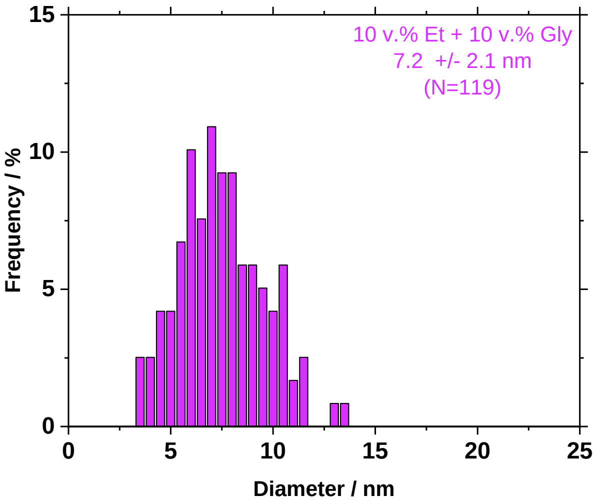
10 v.% Et + 10 v.% Gly
7.2 +/- 2.1 nm
(N=119)
Frequency / %
0
5
10
15
0
5
10
15
20
25
Diameter / nm

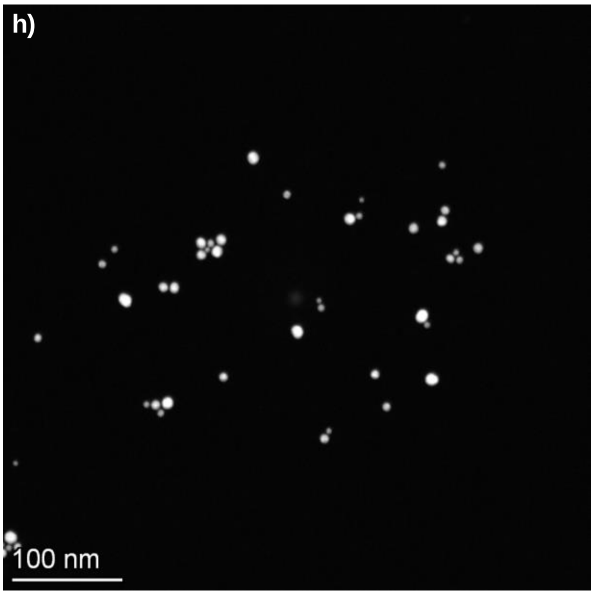
h)
100 nm

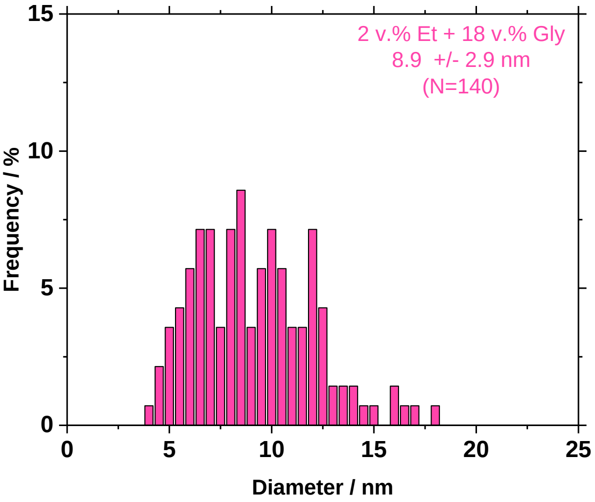
2 v.% Et + 18 v.% Gly
8.9 +/- 2.9 nm
(N=140)
Frequency / %
0
5
10
15
0
5
10
15
20
25
Diameter / nm

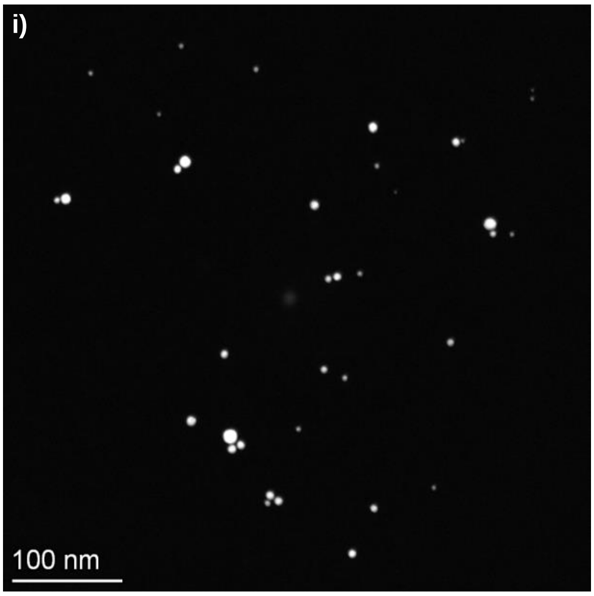
i)
100 nm

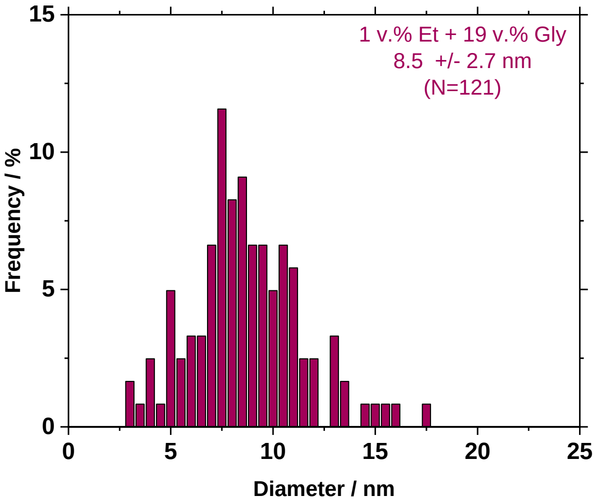
1 v.% Et + 19 v.% Gly
8.5 +/- 2.7 nm
(N=121)
Frequency / %
0
5
10
15
0
5
10
15
20
25
Diameter / nm

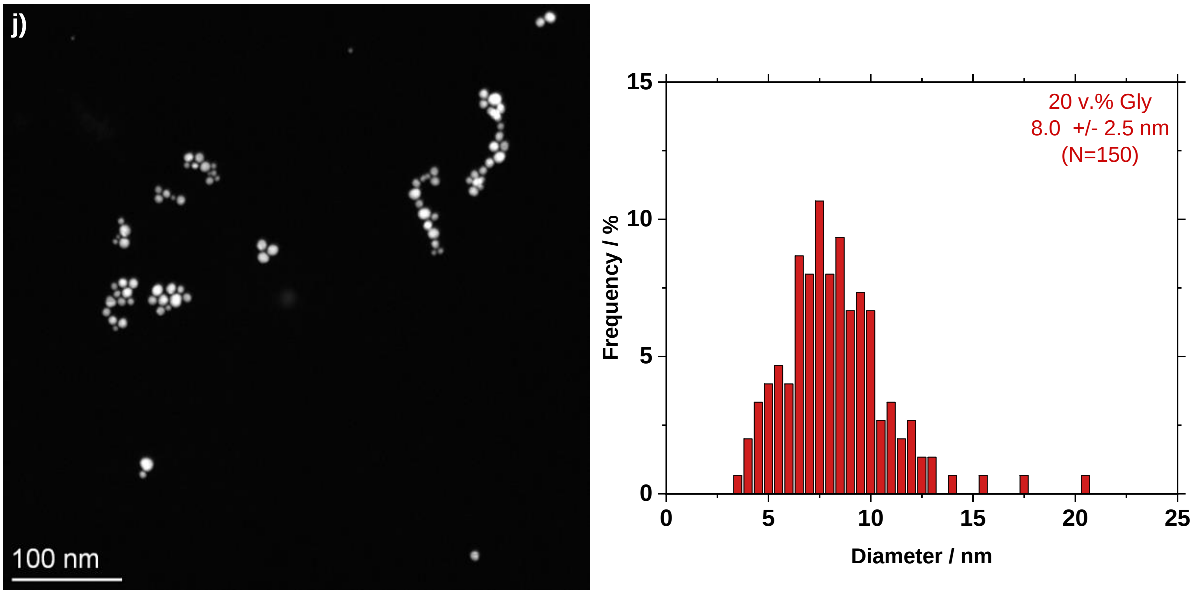
j)
100 nm
20 v.% Gly
8.0 +/- 2.5 nm
(N=150)
Frequency / %
0
5
10
15
Diameter / nm
0
5
10
15
20
25

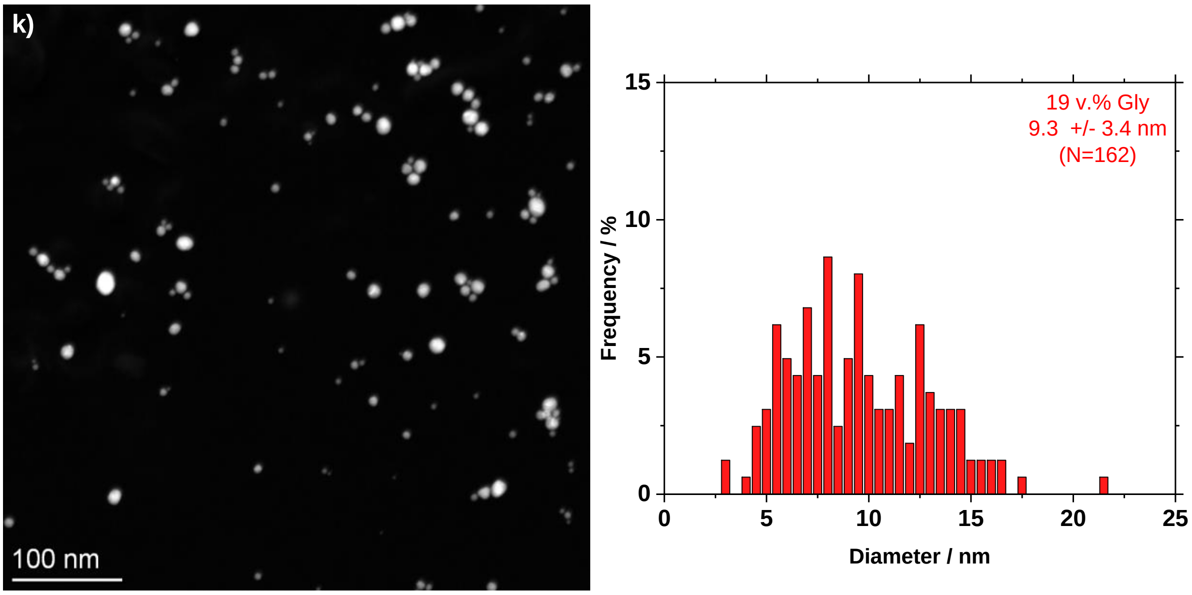
k)
100 nm
19 v.% Gly
9.3 +/- 3.4 nm
(N=162)
Frequency / %
0
5
10
15
Diameter / nm
0
5
10
15
20
25

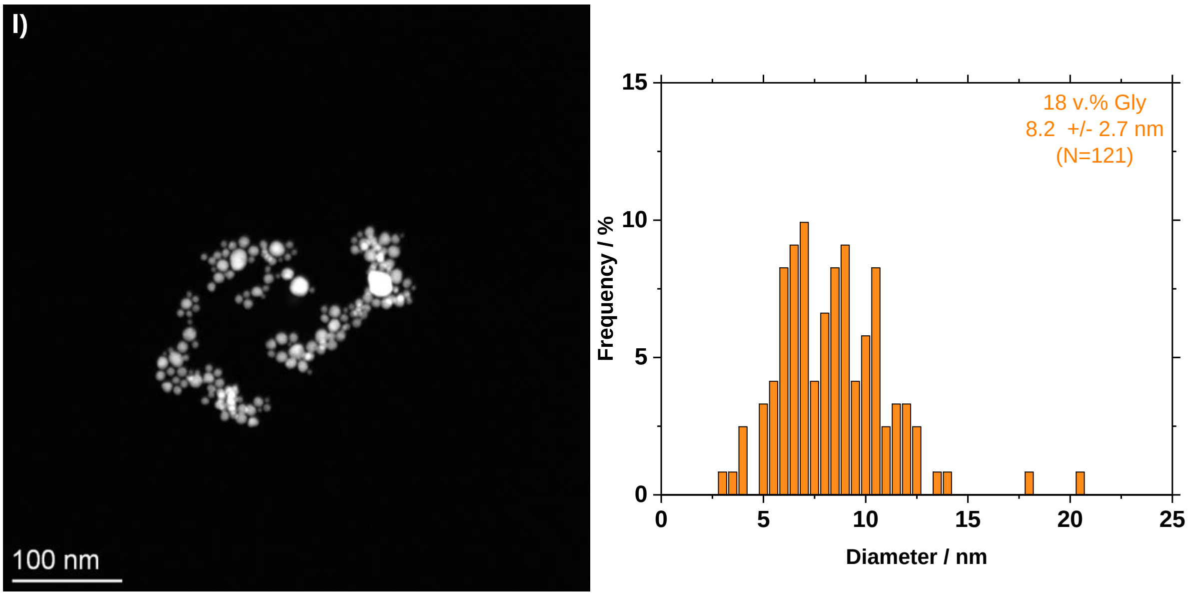
l)
100 nm
18 v.% Gly
8.2 +/- 2.7 nm
(N=121)
Frequency / %
0
5
10
15
Diameter / nm
0
5
10
15
20
25

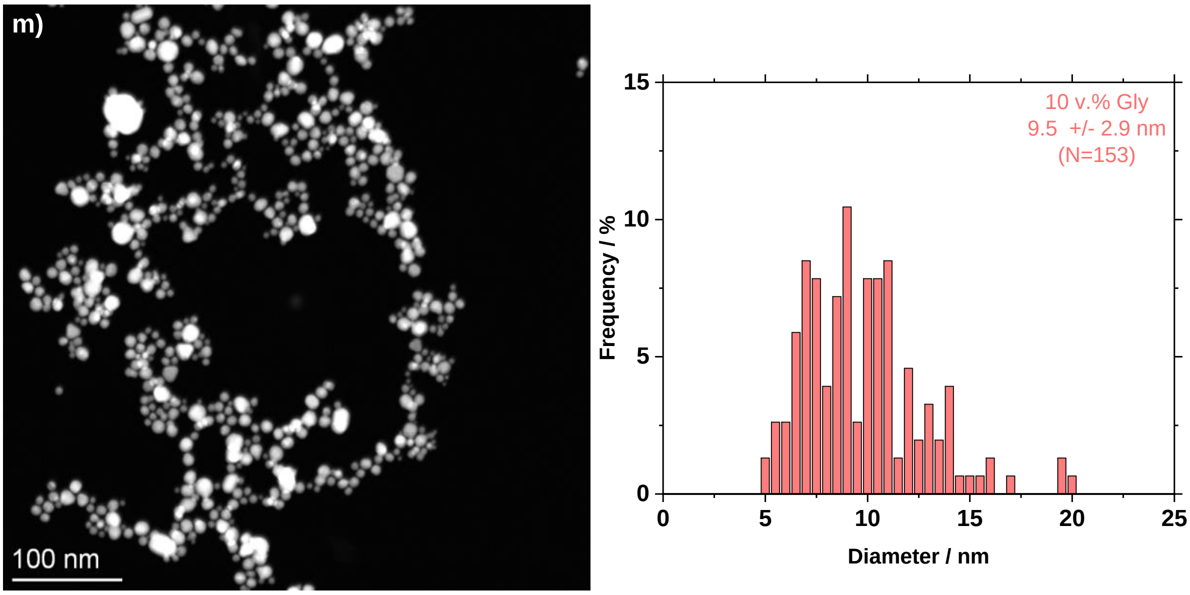
m)
100 nm
10 v.% Gly
9.5 +/- 2.9 nm
(N=153)
Frequency / %
Diameter / nm
0
5
10
15
20
25

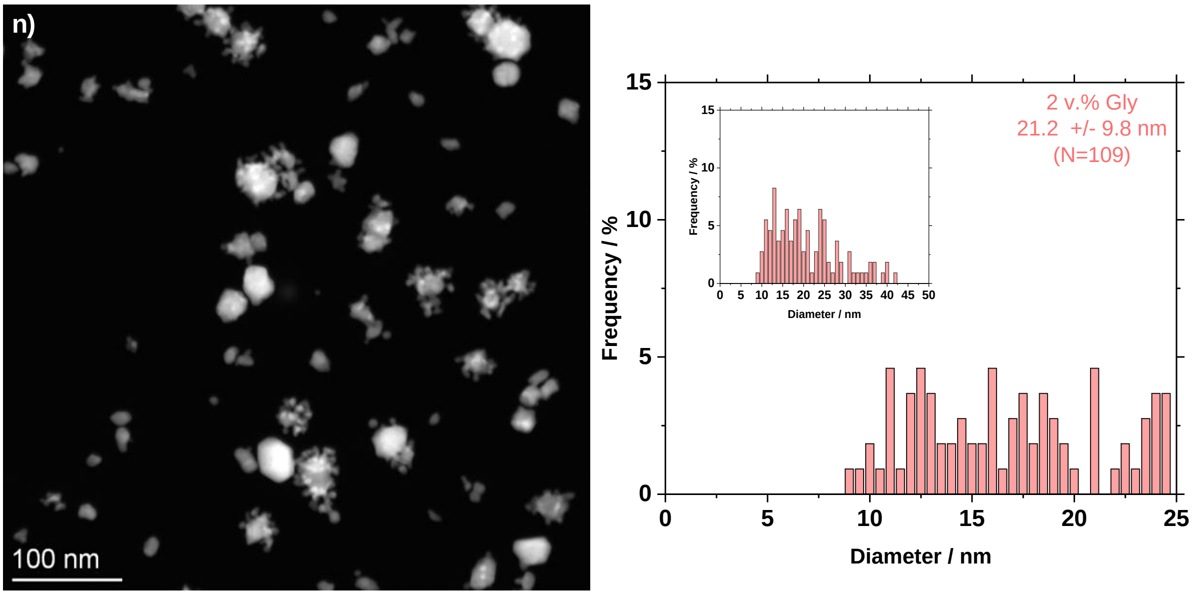
n)
100 nm
2 v.% Gly
21.2 +/- 9.8 nm
(N=109)
Frequency / %
Diameter / nm
0
5
10
15
20
25
30
35
40
45
50

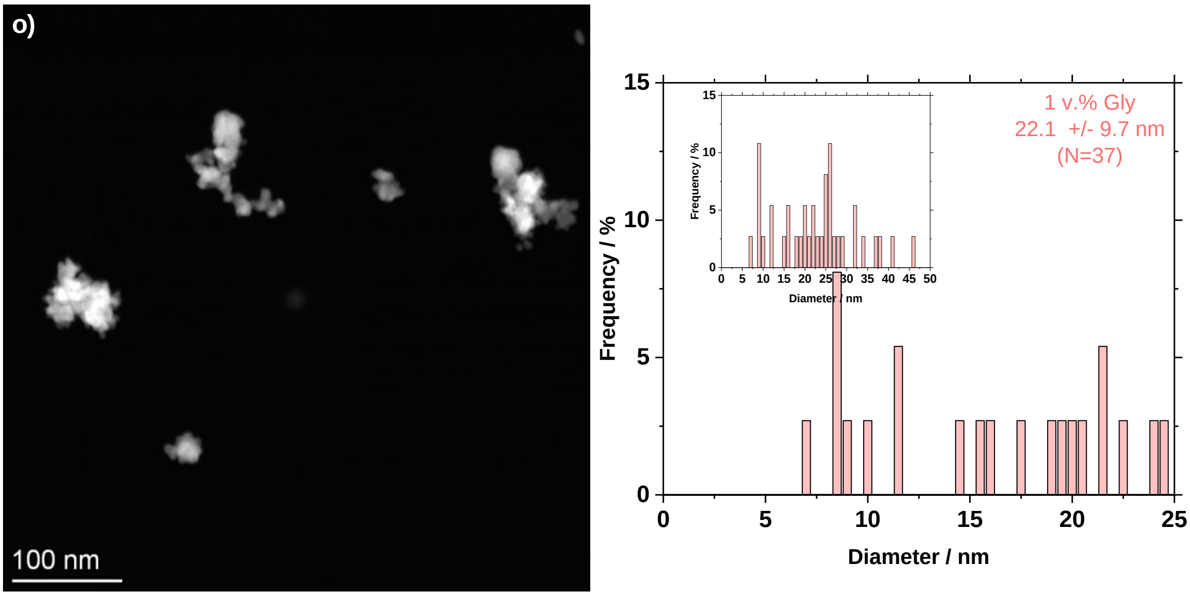
o)
100 nm
1 v.% Gly
22.1 +/- 9.7 nm
(N=37)
Frequency / %
Diameter / nm
0
5
10
15
20
25
30
35
40
45
50

Figure S8. (Left) Illustrative STEM micrograph and (Right) related size distribution for samples obtained using various alcohols contents, as indicated. (a) 10 v.% ethanol, (b) 18 v.% ethanol, (c) 19 v.% ethanol, (d) 20 v.% ethanol, (e) [19 v.% ethanol + 1 v.% glycerol], (f) [18 v.% ethanol + 2 v.% glycerol], (g) [10 v.% ethanol + 10 v.% glycerol], (h) [18 v.% glycerol + 2 v.% glycerol], (i) [19 v.% glycerol + 1 v.% glycerol], (j) 20 v.% glycerol, (k) 19 v.% glycerol, (l) 18 v.% glycerol, (m) 10 v.% glycerol, (n) 2 v.% glycerol, (o) 1 v.% glycerol. Insets are representative of the size distribution for a different size step and a larger X-axis. All experiments were performed with 0.5 mM $HAuCl_4$ and 2 mM NaOH. Et: Ethanol; Gly: Glycerol.

Note that even at low amount of glycerol (1-2 v.%), the reduction happens but is not well controlled. It could be that possible by-products of oxidation that play a role in the stabilization are not formed in quantity high enough to allow stabilization / mono-dispersity.

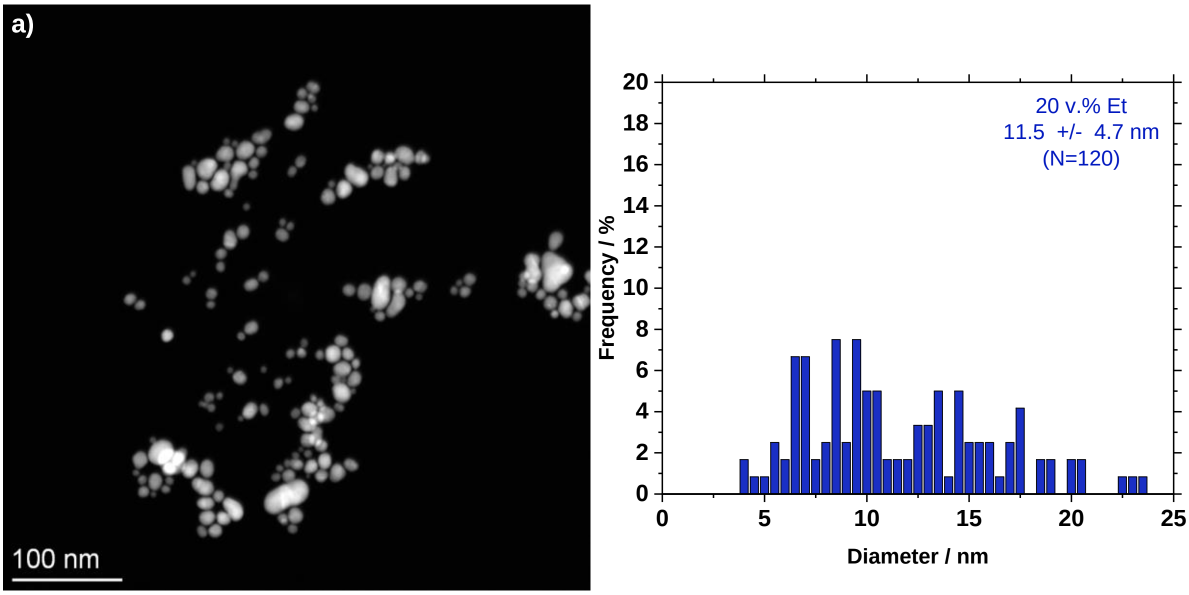
a)
100 nm
20 v.% Et
11.5 +/- 4.7 nm
(N=120)
Frequency / %
0
2
4
6
8
10
12
14
16
18
20
0
5
10
15
20
25
Diameter / nm

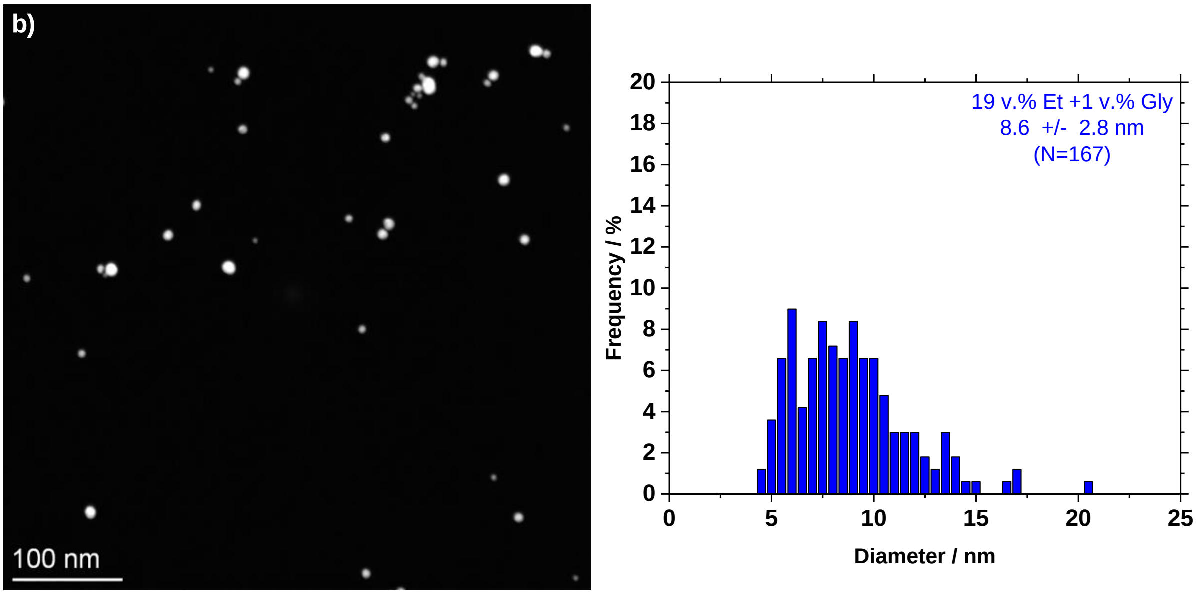
b)
100 nm
19 v.% Et +1 v.% Gly
8.6 +/- 2.8 nm
(N=167)
Frequency / %
0
2
4
6
8
10
12
14
16
18
20
0
5
10
15
20
25
Diameter / nm

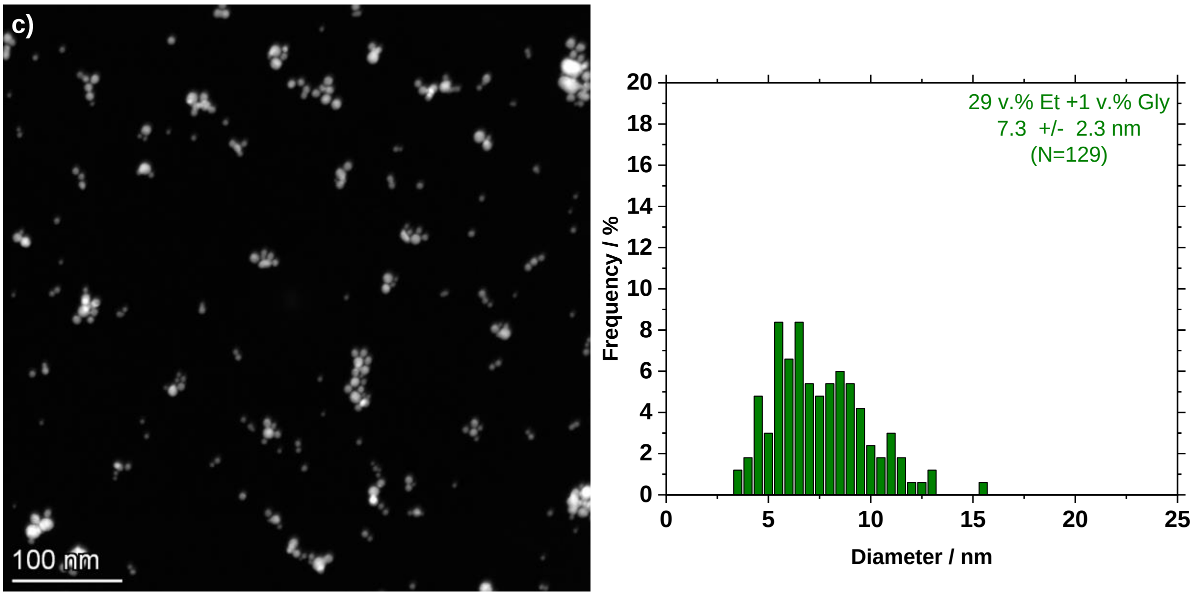
c)
100 nm
29 v.% Et +1 v.% Gly
7.3 +/- 2.3 nm
(N=129)
Frequency / %
0
2
4
6
8
10
12
14
16
18
20
0
5
10
15
20
25
Diameter / nm

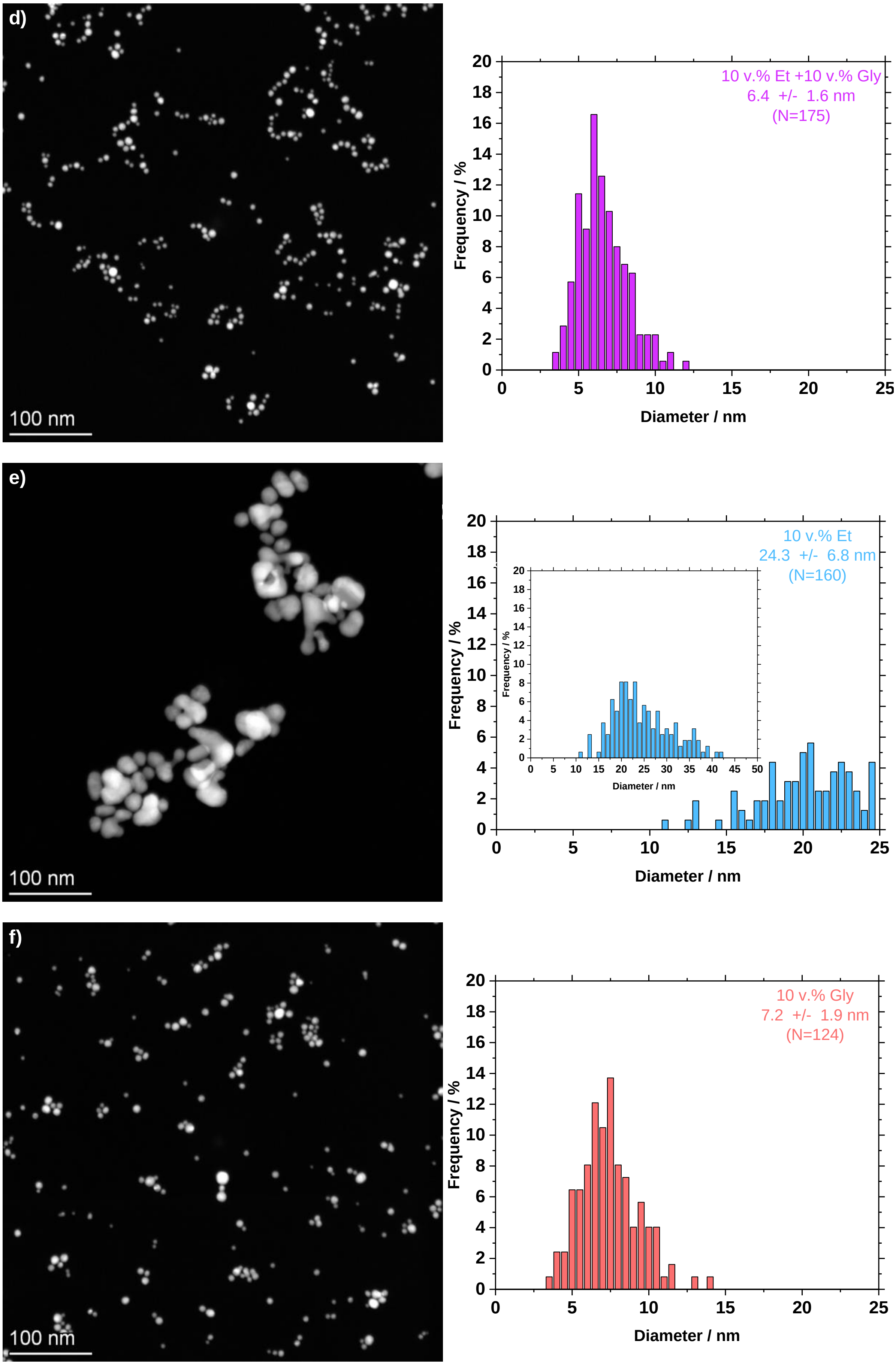
d)
100 nm
Frequency / %
Diameter / nm
10 v.% Et +10 v.% Gly
6.4 +/- 1.6 nm
(N=175)
0
2
4
6
8
10
12
14
16
18
20
0
5
10
15
20
25
e)
100 nm
Frequency / %
Diameter / nm
10 v.% Et
24.3 +/- 6.8 nm
(N=160)
0
2
4
6
8
10
12
14
16
18
20
0
5
10
15
20
25
Frequency / %
Diameter / nm
0
5
10
15
20
25
30
35
40
45
50
f)
100 nm
Frequency / %
Diameter / nm
10 v.% Gly
7.2 +/- 1.9 nm
(N=124)
0
2
4
6
8
10
12
14
16
18
20
0
5
10
15
20
25

Figure S9. Selected STEM data for reproduced experiments (different data set from Figure S8). (Left) Illustrative STEM micrograph and (Right) related size distribution for samples obtained using various alcohols contents, as indicated. (a) 20 v.% ethanol, (b) [19 v.% ethanol + 1 v.% glycerol], (c) [17 v.% ethanol + 3 v.% glycerol], (d) [10 v.% ethanol + 10 v.% glycerol], (e) 10 v.% ethanol and (f) 10 v.% glycerol. Insets are representative of the size distribution for a different size step and a larger X-axis. All experiments were performed with 0.5 mM $HAuCl_4$ and 2 mM NaOH. Et: Ethanol; Gly: Glycerol.

Note that the results in **Figure S8e** and **Figure S9b** differ significantly in the size obtained. This is attributed to the 'too' low amount of glycerol added that can lead to irreproducibility and this is why 2v.% glycerol (with 18 v.% ethanol) was further preferred.

5. Kinetics

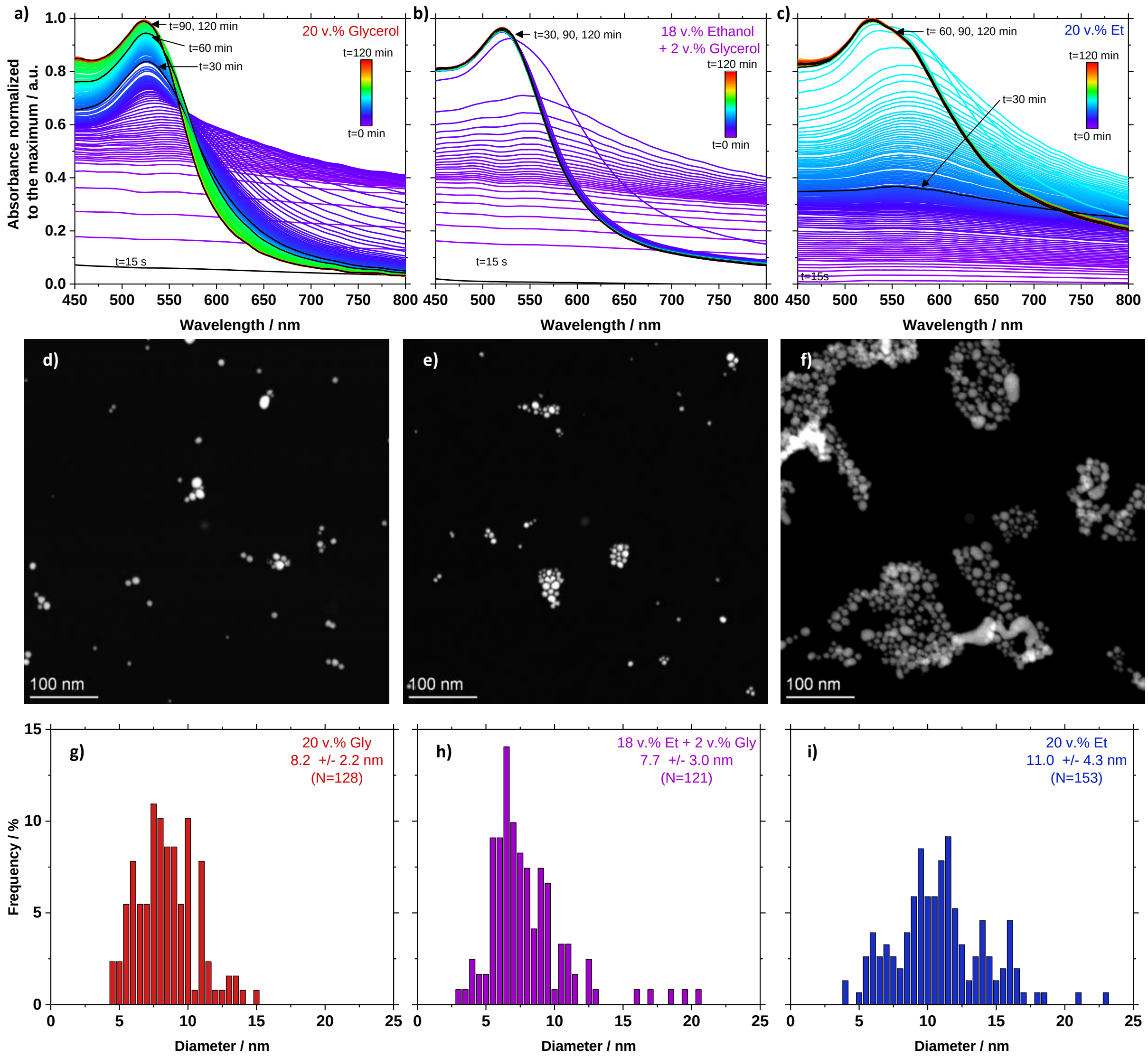

Figure S10. UV-vis spectra as a function of time for syntheses performed with different alcohols: (a) 20 v.% glycerol, (b) [18 v.% ethanol + 2 v.% glycerol] and (c) 20 v.% ethanol, as indicated. The spectra corresponding at times 15 s, 30 min, 60 min and 120 min are highlighted in dark and with arrows. (d-f) STEM micrographs for Au NPs obtained with (d) 20 v.% glycerol, (e) [18 v.% ethanol + 2 v.% glycerol] and (f) 20 v.% ethanol. (g-i) Size distribution for Au NPs obtained with (g) 20 v.% glycerol, (h) [18 v.% ethanol + 2 v.% glycerol] and (i) 20 v.% ethanol. 0.5 mM $HAuCl_4$ and 2 mM NaOH were used in all cases. Et: Ethanol; Gly: Glycerol.

Note that the shoulder present in **Figure S10c** at higher wavelengths was not observed in our previous work [1].The only difference between this work and our previous work is that the light was shone directly on the sample during UV-vis data acquisition. Since we know that dark / darker conditions lead to larger nanoparticles, we attribute the shoulder to the different way to perform the synthesis. Here, the sample is directly in the spectrophotometer so partially in dark conditions in the sense that the sample only receives light from the top (the sides are blocked by the UV–vis spectrophotometer).

Note that this shape with a shoulder was consistently observed by the experimentalist who performed the reactions (in the same way that a shoulder-less spectrum was consistently observed by the experimentalist in previous work [1]).

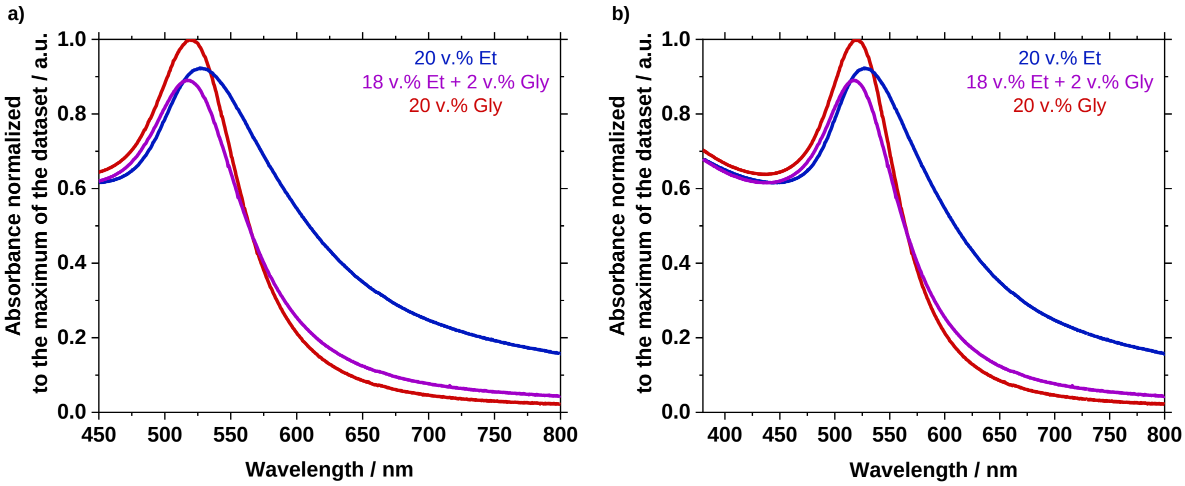

Figure S11. UV-vis spectra after 24 hours for time-resolved UV-vis spectra kinetics experiments for syntheses performed with different alcohols, as indicated. (a) and (b) represent the same dataset with a different X-axis to facilitate the comparison with other data and graphs reported in this work.

The A_{380}/A_{800} metric indicates that the Au NPs obtained with 2 v.% glycerol in 18 v.% ethanol are more stable: Higher A_{380}/A_{800} values for the cases of the mixture compared to 20 v.% ethanol without glycerol with values of 16 and 4, respectively.

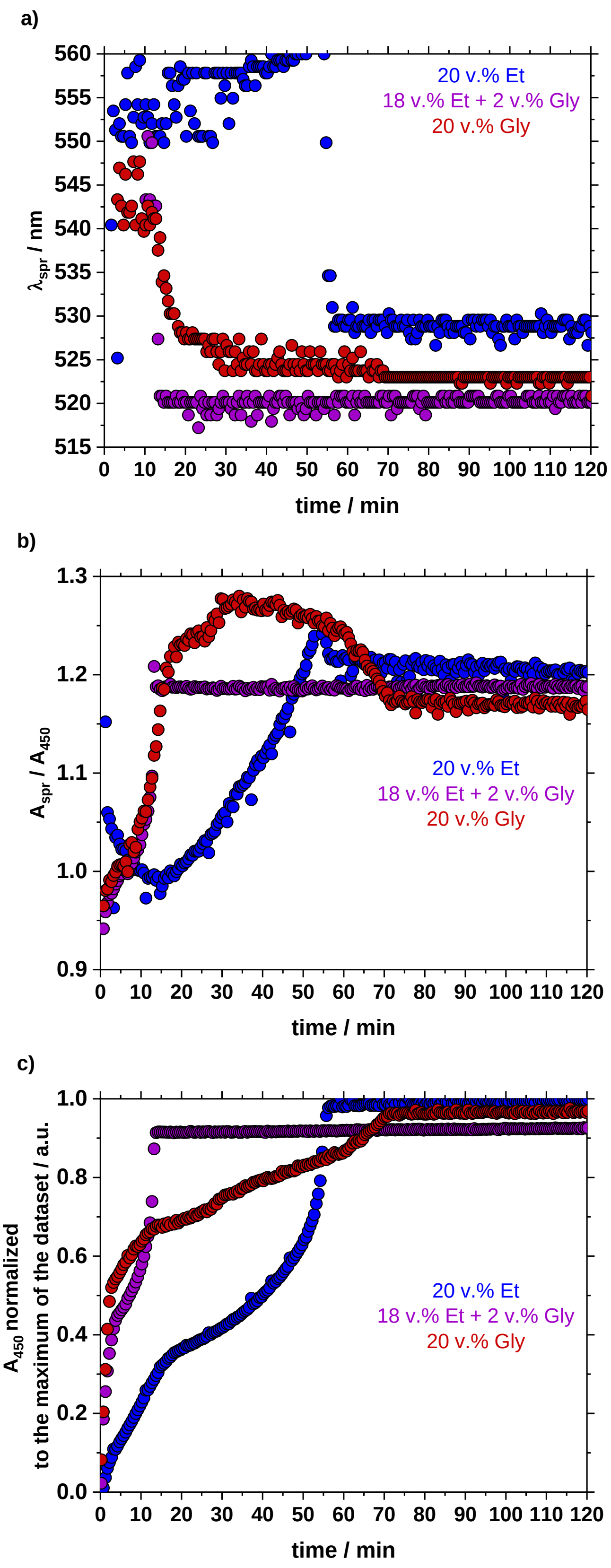

Figure S12. Time-resolved metrics retrieved from UV-vis spectra of kinetics experiments for syntheses performed with different alcohols, as indicated. (a) λ_{spr}, (b) A_{spr}/A_{450} and (c) A_{450} (normalized) as a function of time. 0.5 mM $HAuCl_4$ and 2 mM NaOH were used in all cases. Et: Ethanol; Gly: Glycerol.

Results

Note that the decrease of λ_{spr} values overtime is not related to a decrease in size of the Au NPs but an interaction between formed Au NPs and (depleting) gold precursor [17], **Figure S12a**.

The values at 400 nm or below are not easily retrieved due to the resolution of the UV-vis spectrophotometer and as a proxy for the value at 400 nm the value at 450 nm was used, **Figure S12c**.

Regardless of the metric considered, λ_{spr} as a proxy for size (smaller λ_{spr} values correspond to smaller NP size in most cases, see **Figure S3**), A_{spr}/A_{450} (smaller A_{spr}/A_{450} values correspond to smaller NP size in most cases, see **Figure S3**), A_{450}, as a proxy of A_{400} and therefore a proxy of the NP yield, it is rather clear that (i) glycerol and ethanol-mediated syntheses follow different dynamic and the synthesis is overall slower to lead to Au NPs for ethanol-mediated synthesis vs. glycerol-mediated synthesis, and (ii) adding 2 v.% glycerol to 18 v.% ethanol speeds up the overall formation of the Au NPs in particular in the initial stage.

Note than the different overall shape of the spectra reported in **Figure S10c**, differ from those reported in previous studies [1]. This is attributed to the fact that in a previous study a light was directly shined on the sample during measurement and the samples were not left exposed to the white light of a photobox. Since the samples are here placed in the UV-vis spectrophotometer, it can be anticipated that less light is overall received by the samples, which leads to slower formation of the NPs in particular when ethanol is used. The samples using glycerol or [ethanol+glycerol] are less affected by this change in experimental setup. See further details and discussion below on the influence of light environment in **Figures S13-S14**.

This observation stresses the benefit of small amount of glycerol to improve the *robustness* of the synthesis, for instance to light conditions. These results stress further that controlling the initial stages of the synthesis are key to achieve finer size control in surfactant-free RT syntheses of Au NPs.

6. Importance of controlled light environment and practical considerations

Effects of the light environment. It was previously established that for ethanol-based synthesis (and likely for ethanol-rich mediated syntheses) the light environment can have a strong influence on the outcome of the synthesis [1]: As the wavelength of the light decreases, the NPs are smaller. This was achieved using relatively costly dedicated equipment (specific lamps).

In order to develop simpler and more tunable setups, we investigated the opportunities to use commercially available LED strips (Blue light) to achieve size control of the Au NPs. As reported, in **Figure S6**, the λ_{spr} values are higher compared to experiments performed in a Photobox with white light LED, for various [ethanol+glycerol] contents. The results points towards the fact that Blue light LED strip was not providing enough power and the samples behaved as if they were placed in 'dark' conditions (as per controlled in dark conditions in **Figure S6**).

Those results stress (1) the need for controlled light environment and (2) the need for suitable light source, should one consider developing for instance moveable experimental setup. In this direction, we found that using 60 x 60 x 60 cm boxes as reported here is a suitable option. The synthesis also proceeds well in 40 x 40 x 40 cm photoboxes that are easier to move (e.g. to perform experiments in different laboratory spaces) but present the disadvantage of being smaller and complicate handling of chemicals, e.g. the use of pipettes to inject the gold under stirring and controlled light conditions is more challenging in the smaller space available in the smaller box.

Effects of different containers. The different conditions explored also led us to consider the importance of the containers used for synthesis, as illustrated in **Figure S13**. We compared two types of cuvettes, one with a cut-off around 340-900 nm (UV-vis cuvette) and another one around 230-900 nm in UV-vis (Far UV cuvette) [1]. It was shown using a 365 nm light that the cuvettes with a lower cut-off tend to lead to Au NP colloidal dispersions with lower λ_{spr}. This can be explained by the need for the light to penetrate the material the reactor is made of.

These observations stress the importance of controlled light conditions for successful experiments and account for the possible differences observed in the kinetic experiment reported using 20 v.% ethanol, **Figure S10c**, and those previously reported since the experiments were performed slightly differently [1], as detailed above. Here the samples are simply placed in a photobox, and the sample is surrounded by the UV-vis spectrophotometer, whereas it was previously illuminated directly from above.

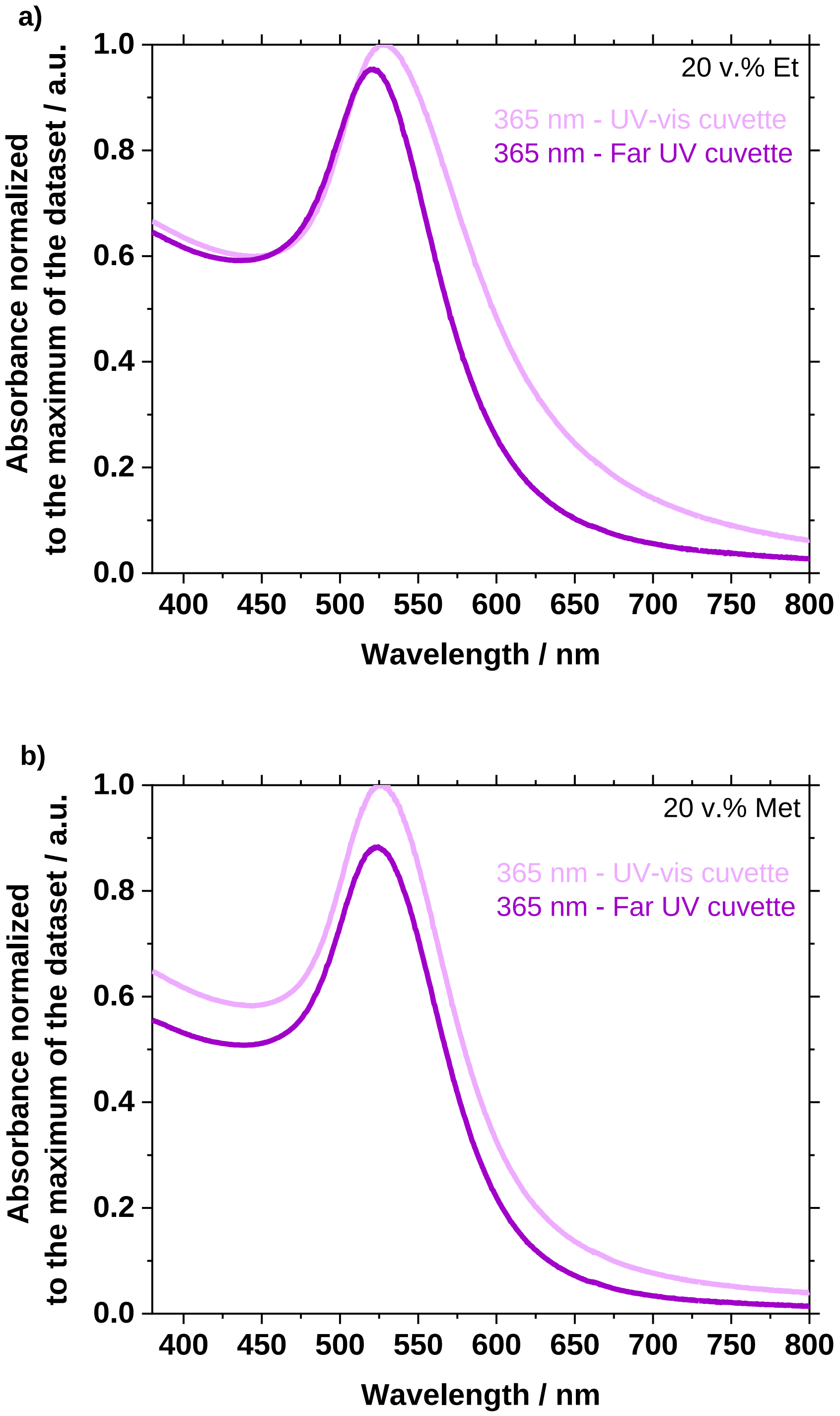

Figure S13. UV-vis spectra for samples prepared with (a) 20 v.% ethanol or (b) 20 v.% methanol under a 365 nm lamp illumination and using two different types of cuvettes as reactors: a UV-vis cuvette and a Far UV cuvette, as indicated and detailed in the text above. 0.5 mM $HAuCl_4$ and 2 mM NaOH were used in all cases. Et: Ethanol; Met: Methanol.

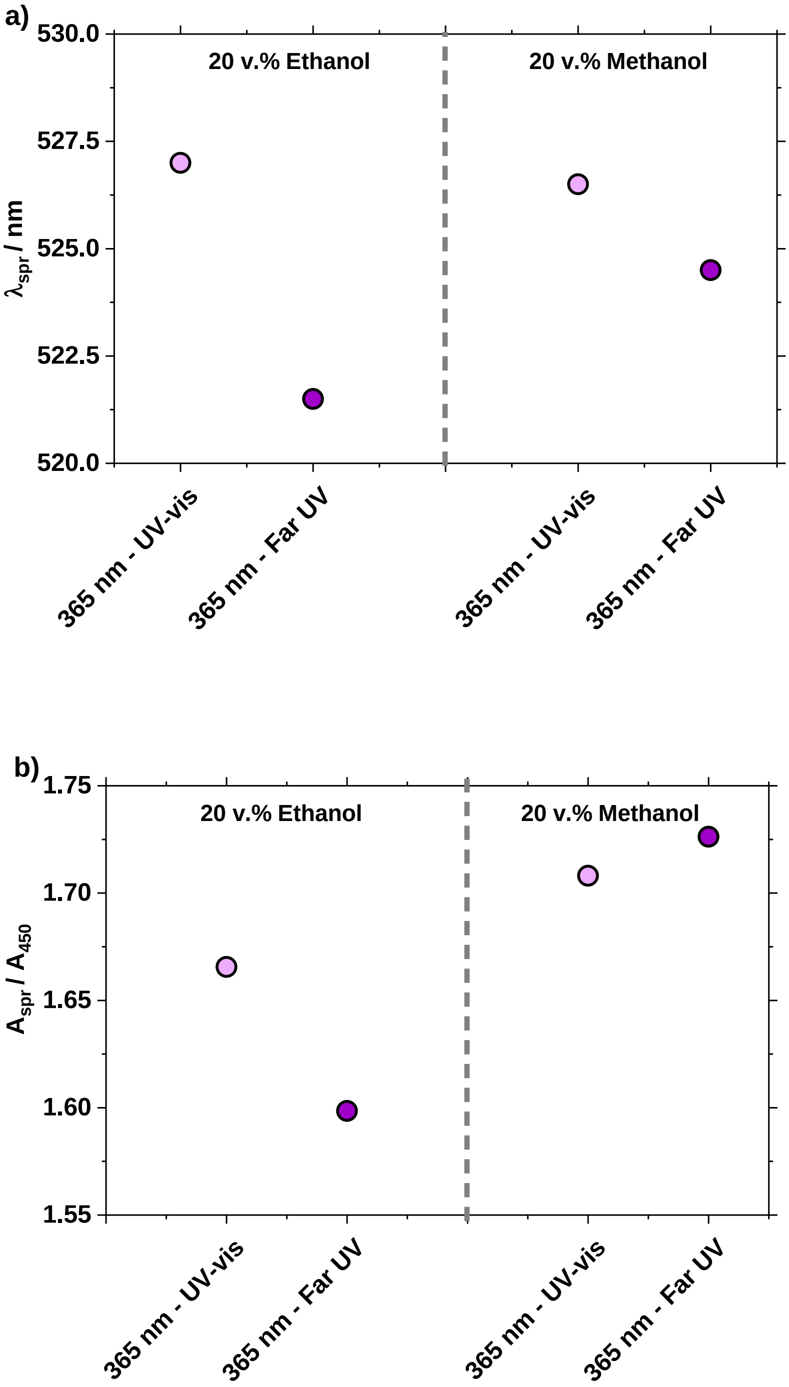

Figure S14. (a) λ_{spr} and (b) A_{spr}/A_{450} values retrieved from UV-vis spectra for samples prepared with 20 v.% ethanol or 20 v.% methanol, as indicated. A 365 nm lamp was used to illuminate the samples and two different types of cuvettes were used as reactors: a UV-vis cuvette and a Far UV cuvette, as indicated and detailed in the text above. 0.5 mM $HAuCl_4$ and 2 mM NaOH were used in all cases.

Those results illustrate the importance of light and choice of container for the experiments. Due to the lower price of the UV-vis cuvettes, those were preferred to the Far UV cuvettes.

7. Optimization

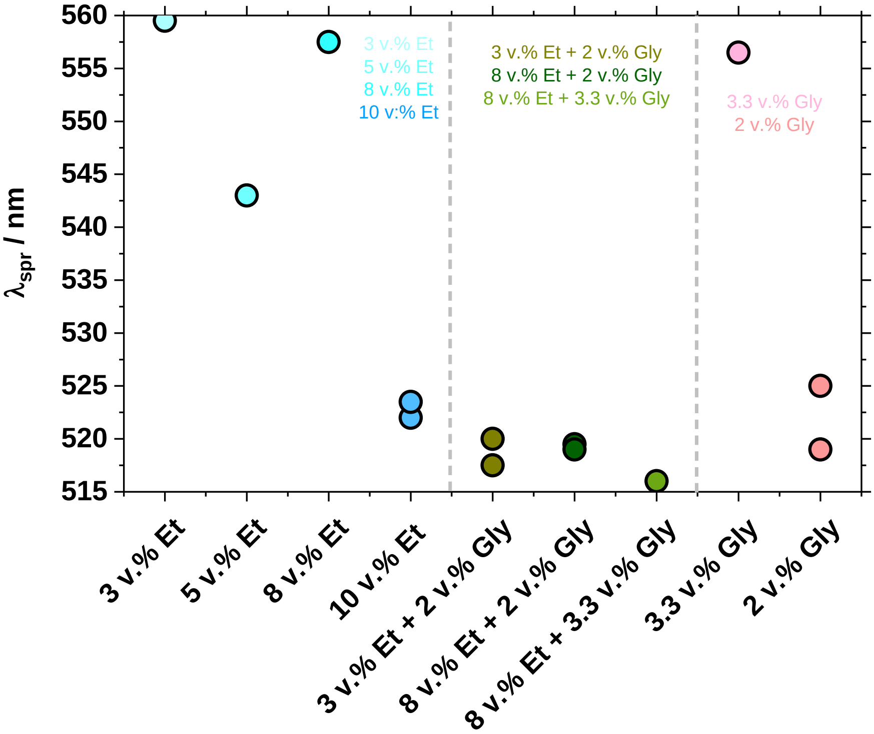

Figure S15. λ_{spr} values retrieved from UV-vis characterization as a function of different alcohol contents and mixtures, as indicated. Et: Ethanol; Gly: Glycerol. In all cases 0.5 mM $HAuCl_4$ and 2 mM NaOH were used.

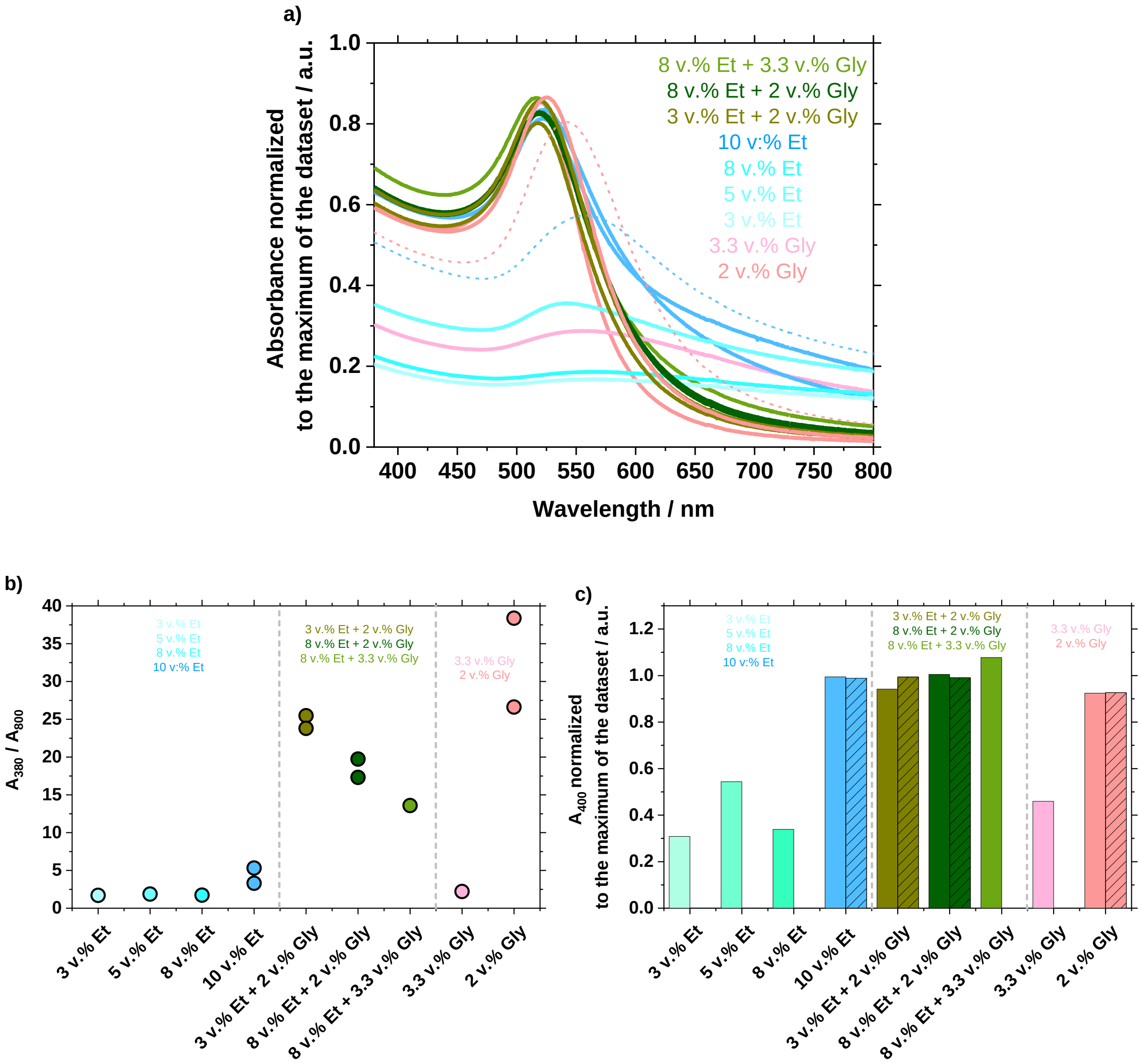

Figure S16. (a) UV-vis spectra for various samples, as indicated, using as source of reducing agent ethanol only, [ethanol+glycerol], or glycerol only in various contents, as indicated. The dashed lines correspond to spectra detailed above to illustrate the more challenging control over the synthesis at low ethanol or glycerol contents. (b) Corresponding A_{380}/A_{800} and (c) A_{400} (normalized) values. To illustrate reproducibility, duplicate of samples prepared using 10 v.% ethanol, [3 v.% ethanol + 2 v.% glycerol], [8 v.% ethanol + 2 v.% glycerol] and 2 v.% glycerol are reported. In all cases 0.5 mM $HAuCl_4$ and 2 mM NaOH were used. Et: Ethanol; Gly: Glycerol.

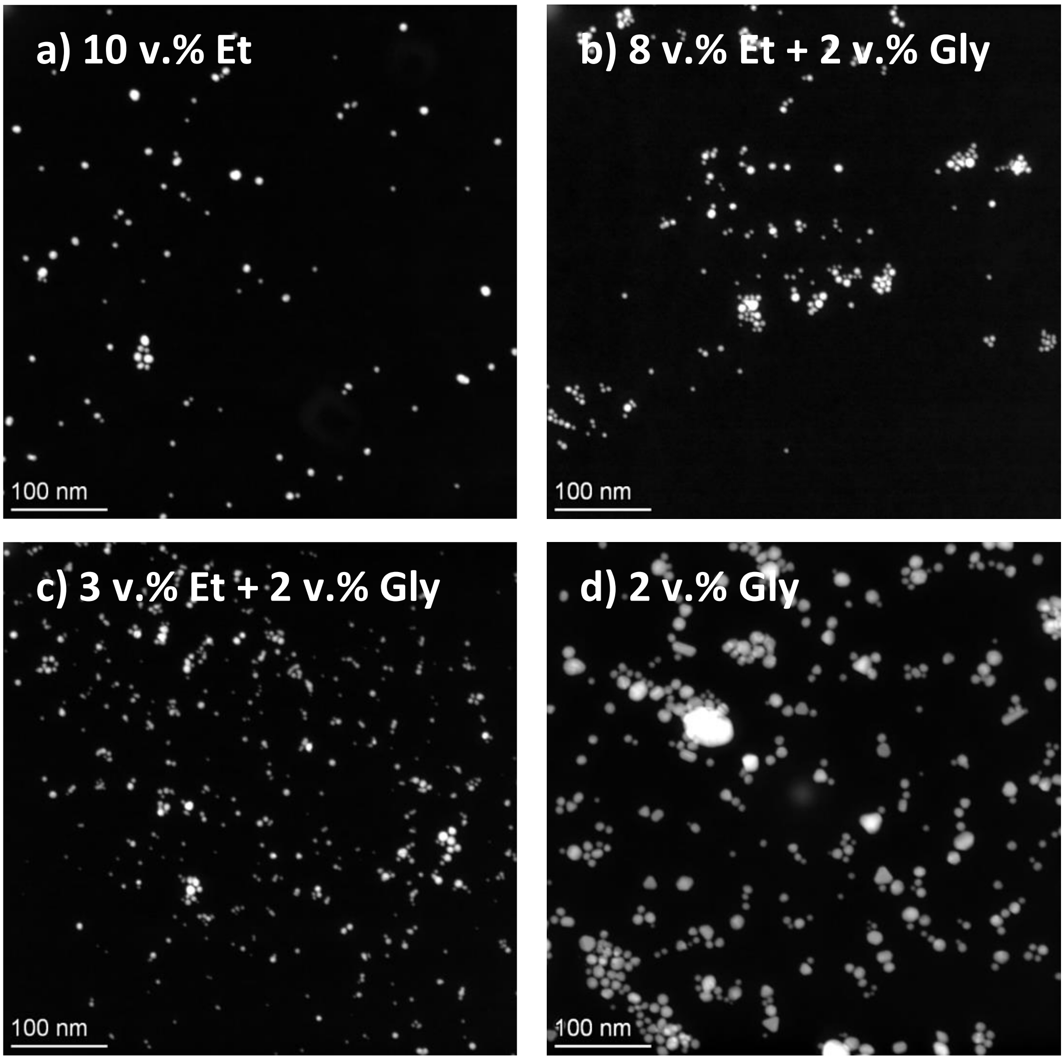

Figure S17. STEM micrographs and related size distribution for samples obtained using (a) 10 v.% ethanol, (b) [8 v.% ethanol + 2 v.% glycerol], (c) [3 v.% ethanol + 2 v.% glycerol] and (d) 2 v.% glycerol. In all cases 0.5 mM $HAuCl_4$ and 2 mM NaOH were used. Et: Ethanol; Gly: Glycerol.

8. Stability

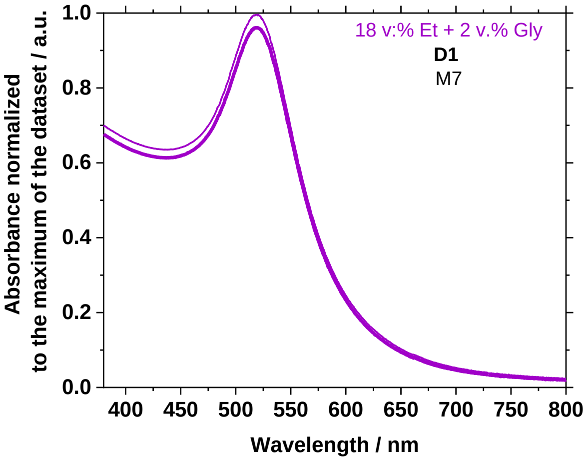

Figure S18. UV-vis spectra for a sample prepared with [18 v.% Ethanol + 2 v.% Glycerol], 24 hours after the beginning of the synthesis (D1) or after 7 months (M7), as indicated. The samples were kept at RT in a drawer. No homogenization was performed. Et: Ethanol; Gly: Glycerol.

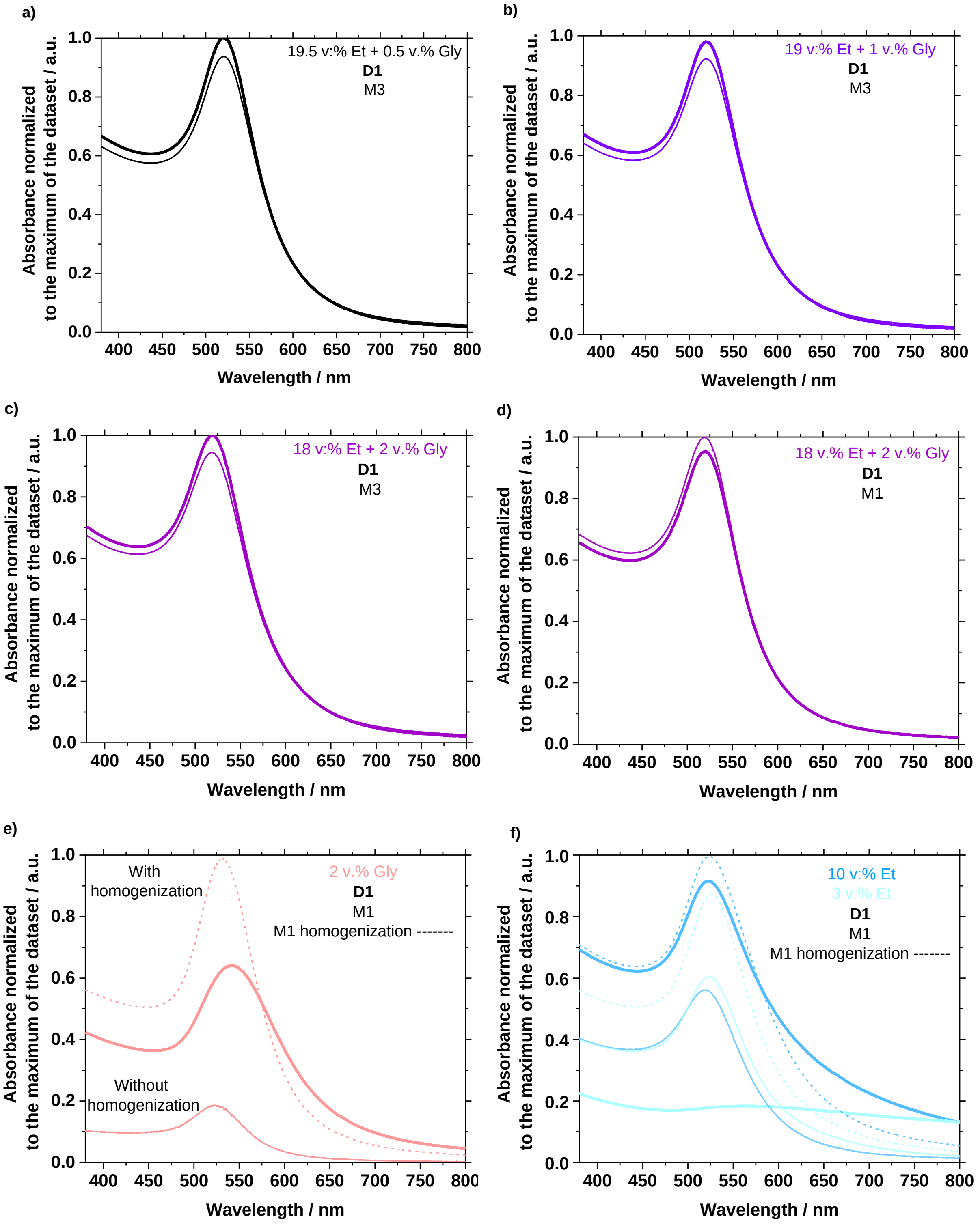
a)
19.5 v:% Et + 0.5 v.% Gly
D1
M3
b)
19 v:% Et + 1 v.% Gly
D1
M3
c)
18 v:% Et + 2 v.% Gly
D1
M3
d)
18 v.% Et + 2 v.% Gly
D1
M1
e)
With homogenization
2 v.% Gly
D1
M1
M1 homogenization -------
Without homogenization
f)
10 v:% Et
3 v.% Et
D1
M1
M1 homogenization -------
Absorbance normalized to the maximum of the dataset / a.u.
Wavelength / nm
0.0
0.2
0.4
0.6
0.8
1.0
400
450
500
550
600
650
700
750
800

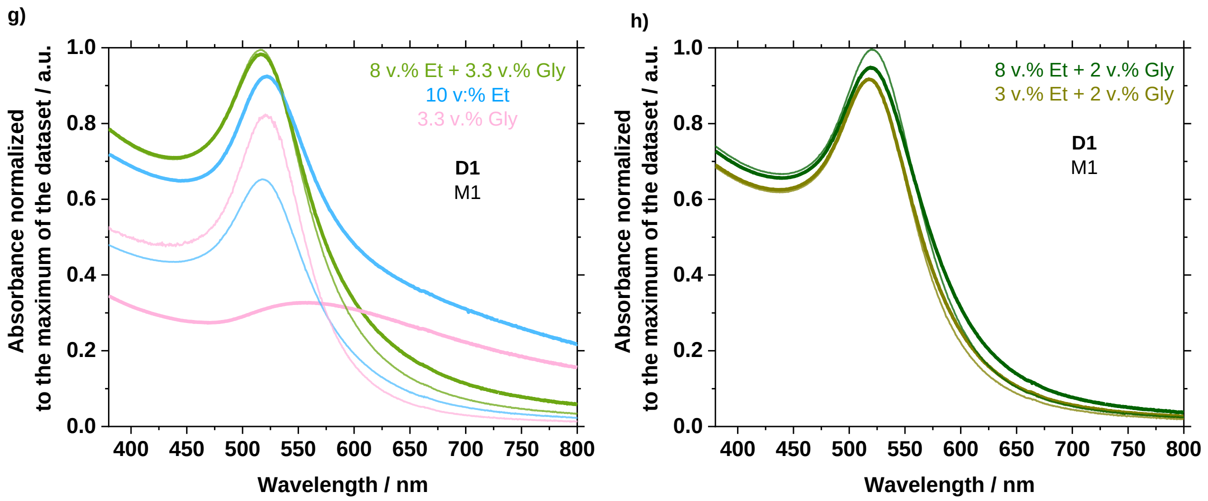

Figure S19. (a-h) UV-vis spectra for different samples, as indicated, 24 hours after the beginning of the synthesis (D1), a month (M1) or 3 months (M3) after the synthesis. Panels (c) and (d) correspond to two different samples. (a-d) correspond to samples in Figures 2-3 in the manuscript and (e-h) to samples related to Figure 5. The samples were kept at RT in a drawer. Measurements were performed without homogenization unless otherwise specified.

Despite the absence of surfactants and the use of low viscosity media, the samples are stable over time even when stored at RT. The small differences observed, e.g. increase of A_{400} value in **Figure S19d** could come from potential solvent evaporation from the 2 mL of solution, despite the fact that the solution was sealed with Parafilm® in capped UV-vis cuvettes. A decrease of A_{400} over time, **Figure S19a-c** is likely due to the sedimentation of the largest NPs since the samples were not homogenized before measurement.

Figure S19e-g illustrates the slow reaction happening with low amount of glycerol (2 v.% and 3.3 v.%) or ethanol (3-10 v.%) where the colloidal dispersions slowly turn red-purple over time and where a better defined spr is observed over time. Using too low amount of ethanol or glycerol only does not lead to reproducible results nor stable colloids, see the overall decrease in absorption in **Figure S19e-g**. These low amounts of alcohols leads to very slow reactions, unstable colloids and sizes larger than for other approaches (based on λ_{spr} values), e.g. compared to cases where a [ethanol+glycerol] mixture is used with comparable glycerol content. In the case of glycerol only or ethanol only, the kinetics are therefore slower than when a [ethanol+glycerol] mixture is used with high ethanol content and similar glycerol content for which a final and relatively more steady state is reached within 24 hours.

Finally, the stability overtime of the slowly forming Au NPs using low amounts of glycerol only is not as good as when [ethanol+glycerol] mixtures are used. For instance in **Figure S19g-h**, homogenization is needed to disperse the NPs prepared with 2 v.% glycerol whereas this is not needed for samples prepared with [18 v.% ethanol + 2 v.% glycerol], [8 v.% ethanol + 2 v.% glycerol] or [3 v.% ethanol + 2 v.% glycerol] as reported in **Figure S18** and **Figure S19c,d,h**.

9. References

1 Rasmussen , D. R., Lock , N. & Quinson , J. Lights on the synthesis of surfactant-free colloidal gold nanoparticles in alkaline mixtures of alcohols and water. *ChemSusChem* **18**, e202400763 (2025). https://doi.org/10.1002/cssc.202400763

2 Quinson, J., Nielsen, T. M., Escudero-Escribano, M. & Jensen, K. M. Ø. Room temperature syntheses of surfactant-free colloidal gold nanoparticles: the benefits of mono-alcohols over polyols as reducing agents for electrocatalysis. *Colloids and Surfaces A: Physicochemical and Engineering Aspects*, **675**, 131853 (2023). https://doi.org/10.1016/j.colsurfa.2023.131853

3 Parveen, R., Ullah, S., Sgarbi, R. & Tremiliosi, G. One-pot ligand-free synthesis of gold nanoparticles: The role of glycerol as reducing-cum-stabilizing agent. *Colloids and Surfaces a-Physicochemical and Engineering Aspects* **565**, 162-171 (2019). https://doi.org/10.1016/j.colsurfa.2019.01.005

4 Varga, M. & Quinson, J. Fewer, but better: on the benefits for surfactant-free colloidal syntheses of nanomaterials. *ChemistrySelect* **10**, e202404819 (2025). https://doi.org/10.1002/slct.202404819

5 Jæger, F., Pedersen, A. A., Wacherhausen, P. S., Smolska, A. & Quinson, J. Surfactant-free gold nanoparticles synthesized in alkaline water-ethanol mixtures: leveraging lower grade chemicals for size control of active nanocatalysts. *ChemRxiv* (2025). https://doi.org/10.26434/chemrxiv-2025-zbs9l

6 Quinson, J. Influence of the alcohol and water grades on surfactant-free colloidal syntheses of gold nanoparticles in alkaline water-alcohol mixtures. *Gold Bulletin* **57**, 27-31 (2024). https://doi.org/10.1007/s13404-024-00345-7

7 Quinson, J. *et al.* Surfactant-free colloidal syntheses of gold-based nanomaterials in alkaline water and mono-alcohol mixtures. *Chemistry of Materials* **35**, 2173–2190 (2023). https://doi.org/10.1021/acs.chemmater.3c00090

8 Quinson, J. Room Temperature Surfactant-Free Syntheses of Gold Nanoparticles in Alkaline Mixtures of Water and Alcohols: A Model System to Introduce Nanotechnology and Green Chemistry to Future Chemists and Engineers. *Journal of Chemical Education* **100**, 3612-3619 (2023). https://doi.org/10.1021/acs.jchemed.3c00492

9 Quinson, J. On the Importance of Fresh Stock Solutions for Surfactant-Free Colloidal Syntheses of Gold Nanoparticles in Alkaline Alcohol and Water Mixtures. *Inorganics* **11**, 140 (2023). https://doi.org/10.3390/inorganics11040140

10 Jensen, T., Saugbjerg, J., Henriksen, M. & Quinson, J. Towards the automation of nanoparticle syntheses: The case study of gold nanoparticles obtained at room temperature. *Colloids and Surfaces A: Physicochemical and Engineering Aspects*, **702**, 135125 (2024). https://doi.org/10.1016/j.colsurfa.2024.135125

11 Freese, T., Elzinga, N., Heinemann, M., Lerch, M. M. & Feringa, B. L. The relevance of sustainable laboratory practices. *RSC Sustainability* **2**, 1300-1336 (2024). https://doi.org/10.1039/D4SU00056K

12 Mourdikoudis, S., Pallares, R. M. & Thanh, N. T. K. Characterization techniques for nanoparticles: comparison and complementarity upon studying nanoparticle properties. *Nanoscale* **10**, 12871-12934 (2018). https://doi.org/10.1039/c8nr02278j

13 Villa, A. *et al.* Characterisation of gold catalysts. *Chemical Society Reviews* **45**, 4953-4994 (2016). https://doi.org/10.1039/c5cs00350d

14 Hendel, T. *et al.* In Situ Determination of Colloidal Gold Concentrations with UV-Vis Spectroscopy: Limitations and Perspectives. *Analytical Chemistry* **86**, 11115-11124 (2014). https://doi.org/10.1021/ac502053s

15 Amendola, V. & Meneghetti, M. Size Evaluation of Gold Nanoparticles by UV-vis Spectroscopy. *Journal of Physical Chemistry C* **113**, 4277-4285 (2009). https://doi.org/10.1021/jp8082425

16 Haiss, W., Thanh, N. T. K., Aveyard, J. & Fernig, D. G. Determination of size and concentration of gold nanoparticles from UV-Vis spectra. *Analytical Chemistry* **79**, 4215-4221 (2007). https://doi.org/10.1021/ac0702084

17 Panariello, L., Radhakrishnan, A. N. P., Papakonstantinou, I., Parkin, I. P. & Gavriilidis, A. Particle Size Evolution during the Synthesis of Gold Nanoparticles Using In Situ Time-Resolved UV-Vis Spectroscopy: An Experimental and Theoretical Study Unravelling the Effect of Adsorbed Gold Precursor Species. *Journal of Physical Chemistry C* **124**, 27662-27672 (2020). https://doi.org/10.1021/acs.jpcc.0c07405

18 Merk, V. *et al.* In Situ Non-DLVO Stabilization of Surfactant-Free, Plasmonic Gold Nanoparticles: Effect of Hofmeister's Anions. *Langmuir* **30**, 4213-4222 (2014). https://doi.org/10.1021/la404556a